CCLAB Composite Construction Laboratory

ÉCOLE POLYTECHNIQUE FÉDÉRALE DE LAUSANNE

Appendix A - Technical Report n° CCLab2000.1b/1

Experiments on Epoxy, Polyurethane and ADP Adhesives

Julia de Castro San Román

Version: March 28th, 2005

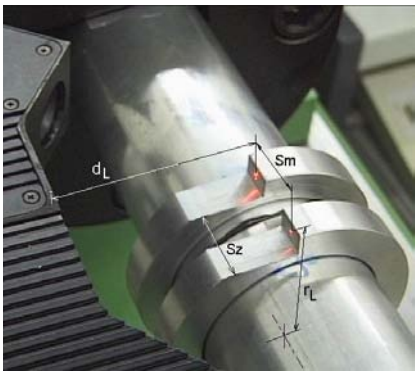

Table of Contents

1 Introduction

1.1 Formulation of the Problem

Joint behavior and joint strength depend on stress distribution within the joint. This stress distribution is influenced by joint geometry and the mechanical properties of the adhesive and adherends. The most significant parameters are: length of overlap, adherend thickness, adhesive thickness, adherend stress/strain behavior and adhesive strain/stress behavior (Matthews et al. 1982). Certain geometric parameter effects - overlap length and adhesive thickness - are dealt with in reports CCLab2000.1a/1 (Vallée and Siebrecht 2001) and CCLab2000.1b/2 (de Castro 2005). Because the aim of this research project is to create ductile joints that develop larger deformations and increase joint strength, adhesives with nonlinear behavior are preferred. An understanding of adhesive behavior is essential for predicting joint deformation and strength. The problem is the lack of reliable data concerning the mechanical properties of adhesives. Since few adhesive manufacturers are currently able to supply the appropriate adhesive mechanical properties of interest to designers, mechanical testing has to be carried out. An extensive variety of standard test methods has been developed by industrial, governmental and research groups, which are updated and revised. The most commonly used are the ASTM (American Society for Testing and Materials), the ES (European Standards) and the ISO (International Standards Organisation) standards. Adams, Comyn and Wake (1997) present a brief overview.

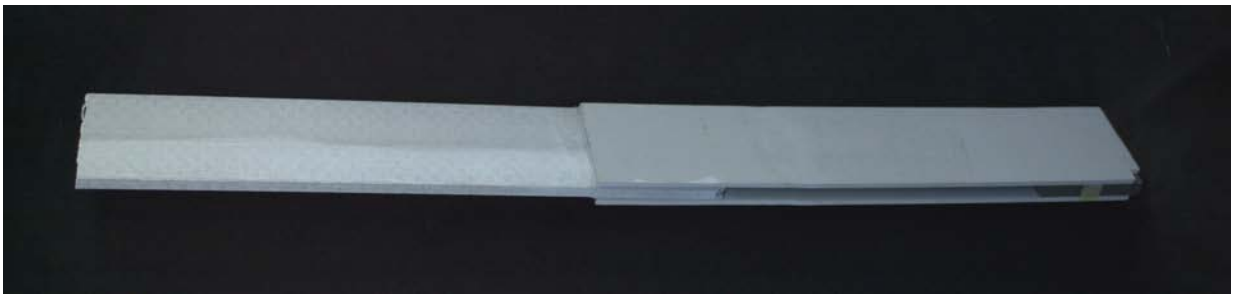

Figure 1 Adhesively-bonded double-lap joint

Intrinsic mechanical characteristics can be measured in two ways:

- on the bulk adhesive material;
- on adhesively-bonded joints, in the thin layer form;

using a static or dynamic testing method. The testing of bulk specimens, comparable to that of plastic materials, determines adhesive properties without any influence from the adherends. These properties are obtained under a uniform and uniaxial state of stress. Specimens may be tested in uniaxial tension or compression, flexion and torsion. The testing of bulk specimens is easier than that of adhesive layers because the elastic deformations are larger and can therefore be measured more accurately using standard extensometers or strain gages. The most difficult part is to manufacture specimens without

defects such as voids and porosity since air bubbles trapped during mixing are difficult to remove if the adhesive is very viscous or has a short pot-life.

The testing of adhesively-bonded joints must be correctly planned to ensure a uniform and uniaxial state of stress in the adhesive layer. Specimens are usually in the form of a cylindrical butt joint to which an axial load or a torque is applied, or in the form of a thick adherend joint loaded in tension. The main difficulty is the accurate measurement of the small displacements across the adhesive.

For a long time, researchers thought that bulk adhesive properties were different from adhesive properties in the joint. It was believed that the elastic modulus increased with reduction of adhesive thickness but this was due to incorrect interpretation of experiments (Adams et al. 1997). Nevertheless, Adams and Coppendale (1977) showed that the layer and bulk mechanical properties are similar under the same curing conditions. The problem is to provide the same curing conditions for bulk and layer because of runaway exothermic reactions in bulk forms, which can explain discrepancies. In his study of five epoxy adhesives, Jeandrau (1986; 1991) confirmed that good correlation exists between the properties of adhesive in bulk forms and those of the adhesive layer between the adherends. This conclusion had already been reached by Althof and Brockmann (1976) and Ishai and Dolev (1981a and 1981b). It should be borne in mind that correlation between bulk and layer properties depends on the quality of bulk specimens without defects, such as voids and porosity, since the contents and size of defects are generally smaller in layer than in bulk specimens (Tong and Steven 1999).

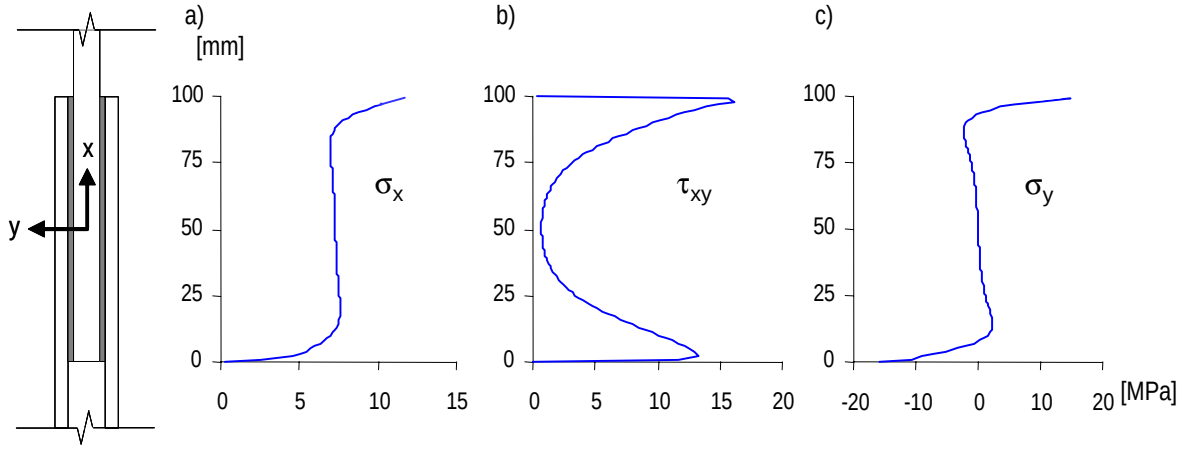

Figure 2 (a) Axial, (b) shear and (c) through-thickness stress distribution along the overlap length of adhesively-bonded double-lap joint (5 and 10 mm thick GFRF laminates from Fiberline Composites S/A connected with a 2 mm thick layer of SD330 epoxy adhesive from SIKA AG)

The stress-strain curve for an adhesive varies according to the operating environment, with both temperature and rate of loading. In general, an increased rate of loading has an equivalent effect to reduction of temperature upon properties such as elastic modulus and yield stress. This increases the stiffness and reduces the ductility of the adhesive. Nonetheless, the strain energy, proportional to the area under each stress-strain curve, remains similar (Hart-Smith 1990). This dependence of properties upon rate of loading and temperature is also found in visco-elastoplastic materials. Thus, the

estimation made with bulk properties could differ from adhesive joint behavior because of differences in operating environment.

In contrast to metal joints, GFRP joints usually fail in the adherend rather than in the adhesive layer. Nevertheless, adhesive behavior must be identified since it influences the load transfer in the joint, and then ultimate failure in the adherends. The adhesive layer is subjected to a complex stress state (Figure 2). This can be related to available stress-strain data by evaluation of an "effective" uniaxial tensile stress equivalent to the combined state of stress. The state of stress may be obtained by superposing the hydrostatic and deviatoric stresses (Figure 3) (Adams and Coppendale 1979). The hydrostatic stress component, also called second stress invariant, is the mean of the three normal stresses while the deviatoric stress component, also called the first stress invariant, is the normal stress reduced by the value of the hydrostatic stress component. The hydrostatic stress component tends to change the volume of the material, but not its shape, since all the faces of the element are subjected to the same stress. The deviatoric stress component tends to change the shape of the element of material, or distort it, but not its volume. For ductile isotropic materials, the "effective stress" depends on the deviatoric component of stresses. This is the case for the commonly known functions postulated by Tresca and von-Mises. However, for adhesives and all polymers, it has been found that effective stress depends on the deviatoric component of stresses and the hydrostatic component of stresses. This is due to a significant difference between the stress-strain curves and yield stress level under uniaxial tension and uniaxial compression loading (Ikegami et al. 1979). Various von-Mises modified functions have been developed: the first one was adapted from Raghava and Caddell (1973) by Peppiatt (1976) and another one has been presented by Gali et al. (1981). Both include the ratio between the compressive and tensile yield stress or strength values.

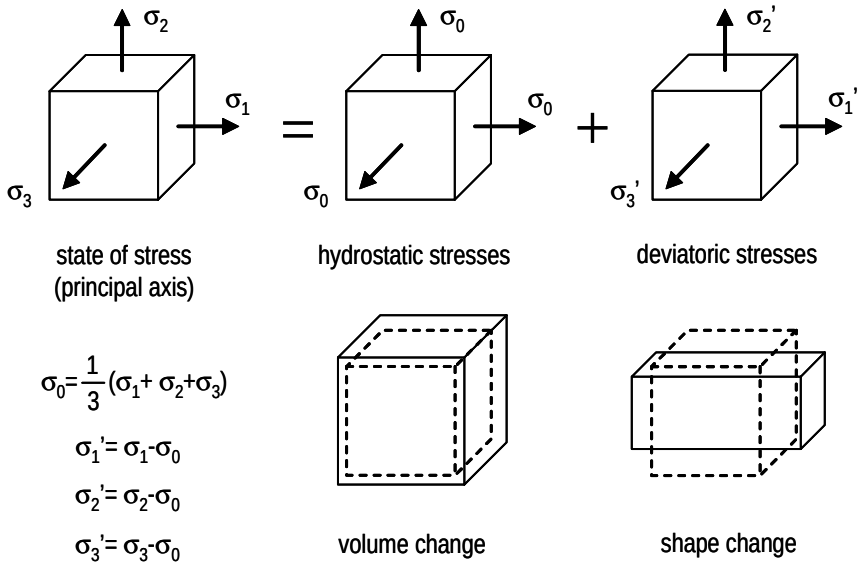

Figure 3 Hydrostatic and deviatoric stress components and associated material changes

The test series presented here deals with determination of the mechanical properties of adhesives in tension, compression and shear.

1.2 Objectives

To determine the mechanical properties of three adhesives used for joining pultruded GFRP elements (de Castro 2004), different tests were carried out in collaboration with the adhesive supplier and partner, SIKA AG, and the Department of Strength and Technology of the EMPA in Dübendorf, Switzerland.

The test series have three main objectives:

- determination of the stress-stain curves in tension, compression and shear, to introduce them in analytical and/or FEA models;
- comparison of adhesive properties;
- determination of the adhesive suitable for the development of ductile joints.

1.3 Experimental Program

Three adhesives are considered in the research program: the epoxy resin SD 330, the polyurethane adhesive S-Force 7851 and the adhesive SikaFast 5221 based on ADP technology. These adhesives are produced by SIKA AG; reasons concerning their choice are explained in 1.4.

The test program consists of a series of 3-5 test specimens per adhesive type:

- tensile tests according to EN ISO 527 (1996), quasi-static, destructive testing (Chapter 2);
- compressive tests according to ASTM D 695-96 (1996), quasi-static, destructive testing (Chapter 3);
- shear tests designed at the EMPA, similar to the former EN ISO 11003-1 type, quasi-static, destructive testing (Chapter 4).

Additional tensile tests with loading-unloading-reload cycles were carried out on the ADP adhesive to quantify visco-elastoplastic behavior.

The compressive tests were carried out on August 30, 2001 and tensile tests were carried out between 2001 and 2004 in the laboratory of SIKA AG, Zurich. Shear tests were carried out during April 2002 in the Department of Strength and Technology of the EMPA.

1.4 Adhesive Choice and Adhesive Characteristics

The three adhesives considered in the research program are resins rather than adhesive films since adhesive thickness can vary and thus compensate for the lack of flatness of adherends. An appropriate viscosity is required to guarantee easy application. The adhesives considered (Figure 4) are:

- the cold-cured two-component epoxy resin SD 330, designated EP in this project;
- the cold-cured two-component polyurethane adhesive S-Force 7851, designated PU;
- the fast-curing two-component adhesive SikaFast 5221 based on ADP technology, designated ADP.

The SD 330 is a resin developed for impregnation of carbon fiber-fabrics used for strengthening purposes. It offers high strength and stiffness but presents brittle failure. As epoxies are commonly used for structural bonding, it seems worthwhile to compare their behavior with new adhesives chosen for the same application.

Since the aim of the project is to create ductile joints that develop larger deformations and increase joint strength, adhesives with nonlinear behavior are preferred. The S-Force 7851 was developed for structural bonding of car body parts made from carbon-fiber reinforced epoxy resins. It is more flexible and ductile than the epoxy. The SikaFast 5221 adhesive, based on ADP (Acrylic Double Performance) technology, was developed specially for structural bonding. ADP technology offers a new generation of fast-curing soft adhesives designed to substitute welding and mechanical fastening techniques. It is very flexible and ductile.

a) b) c)

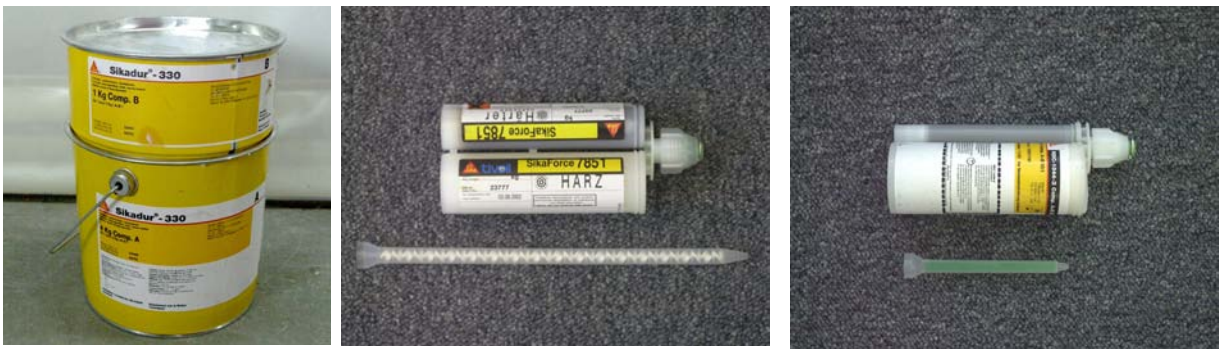

Figure 4 (a) SD 330; (b) S-Force 7851 and (c) SikaFast 5221 in a cartridge useful for small series (215 ml and 250 ml) and a suitable mixer tube

The following table shows some technical data; more information is available at www.sika.ch.

Table 1 Adhesive technical characteristics

Adhesive	SD 330	S-Force 7851	SikaFast 5221
Chemical base	two-component epoxy resin	two-component polyurethane adhesive	two-component acrylic-based adhesive
Supplier	Sika	Sika	Sika
Glass transition temperature T_g[1]	+45°C (23°, 7 days cured)	+40 °C	+52°C (23°, 1 day cured)
Consistency	thixotropic	thixotropic	thixotropic
Cure	ambient temperature	ambient temperature	ambient temperature
Working time [2]	40 min at +23°C	15 min at +25°C	9 min at +23°C
Application temperature (environment and supports)	+10°C to +25°C	+15°C to +100°C	+10°C to +40°C

[1] supplier data
[2] maximum allowable period between after the mixing of components in which joint must be assembled

2 Tensile Tests

2.1 Tensile Test Choice

The butt joint loaded in uniaxial tension appears to ensure a uniform and uniaxial state of stress in the adhesive layer. Nevertheless, Adams and Coppendale (1977, 1979) and Jeandrau and Grolade (1985) have shown that tensile stress distribution is not uniform due to the Poisson's ratio and possible misalignment of the two thin-walled tubes (Figure 5(a)). The situation is complicated by the constraint applied to the adhesive by the adherends. Without this constraint, the radial strain in the adhesive is greater than that in the adherends because the Young's modulus of the adhesive is much lower than that of the adherends. The adherends limit this radial strain and induce radial and circumferential tensile stresses in the adhesive. The apparent Young's modulus determined with the test method is related to the true Young's modulus (Adams and Coppendale 1977).

The bulk adhesive specimens are not susceptible to these problems and are more suitable for providing reliable data. The most difficult part is to produce specimens without defects (voids and porosity). Typical tensile bulk specimens have a "dog-bone" form (Figure 5(b)). Crocombe et al. (1993) present a simple four-point bending test that determines, simultaneously, both the tensile and compressive stress-strain behavior of a bulk adhesive and the ratio between compressive and tensile stress (Figure 5(c)).

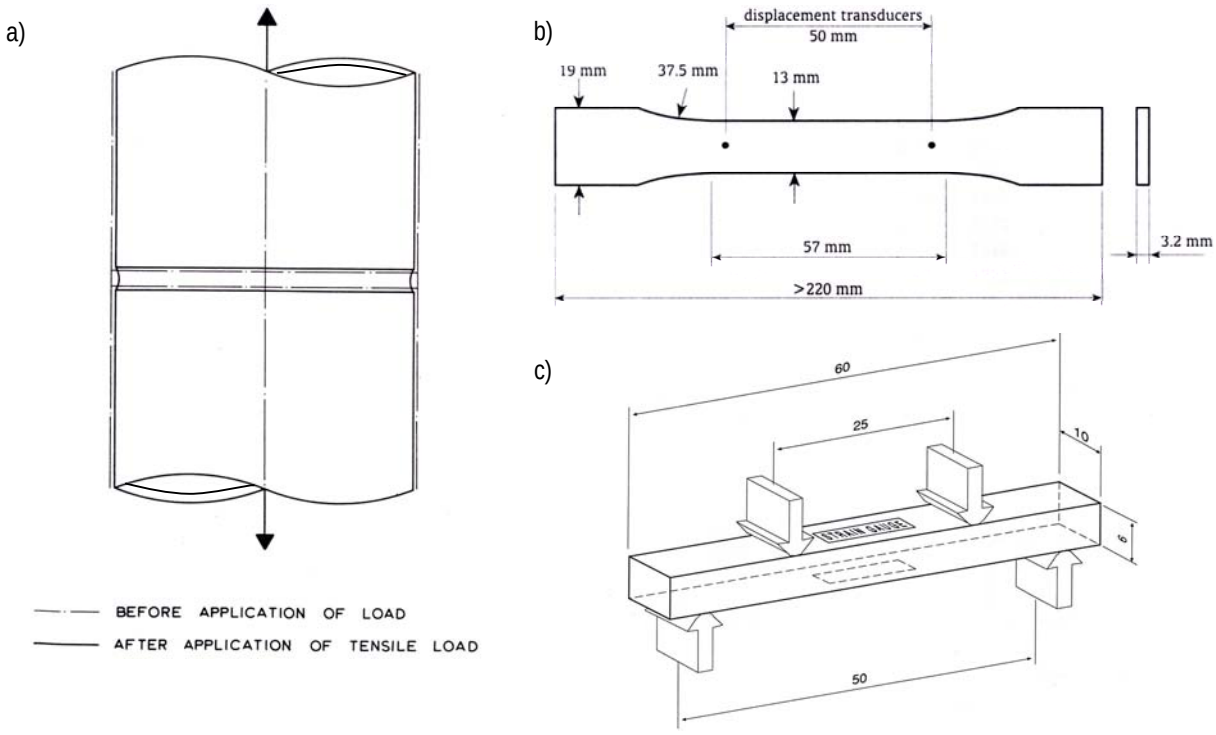

Figure 5 (a) Tensile butt joint specimen (Adams and Coppendale 1977); (b) Tensile bulk specimen according to ASTM D638-96 (1996); (c) Four-point bend bulk specimen (Crocombe et al. 1993)

The tensile adhesive bulk test is preferred to the butt joint, as it provides a stress-strain curve and therefore tensile Young's modulus, Poisson's ratio, elastic limit and failure characteristics.

2.2 Test Specimens

2.2.1 Dimensions

For each of the three adhesives, five tensile test specimens (as shown in Figure 6) were prepared according to EN ISO 527-2 and tested. The EP and PU specimens were manufactured according to type 1A and the ADP specimens according to type 5A. The choice of specimen type depends on adhesive stiffness; larger specimens are required for stiff adhesives due to their low deformations and the manufacturing process (see 2.2.2). The specimens have a prismatic form with reinforcement at the ends to avoid grip failure. The transition is made with a constant radius of 25 mm for specimens 1A and two successive constant radii, 12.5 mm and 8 mm, for specimens 5A.

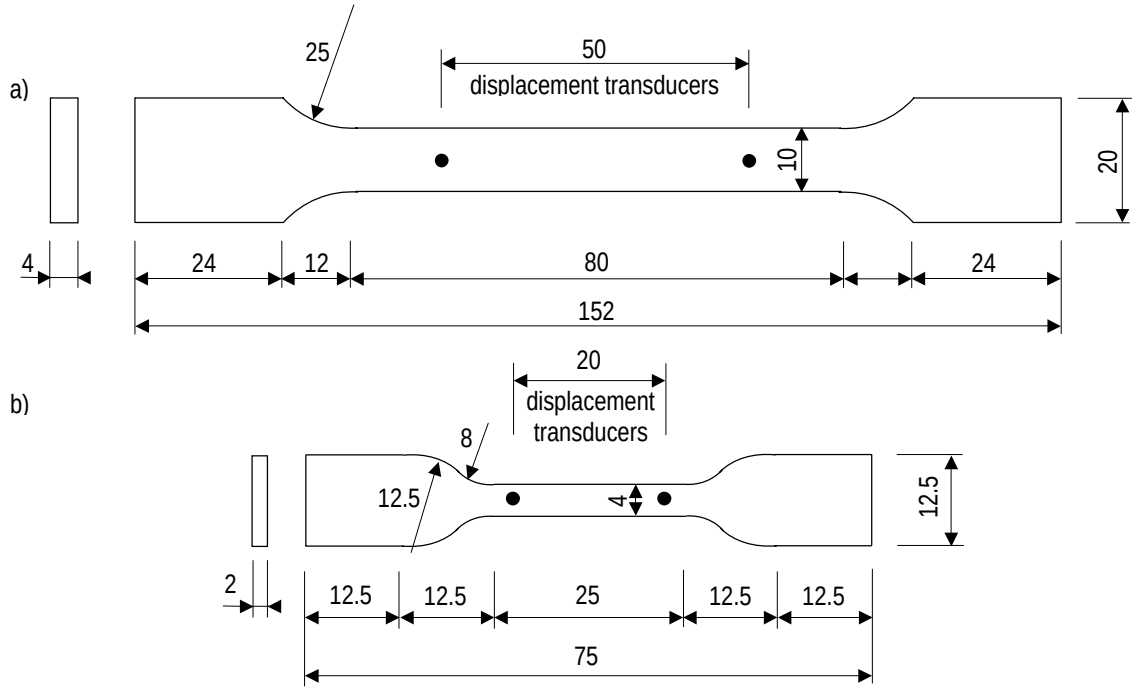

Figure 6 Dimensions of the tensile test specimen according to EN ISO 527-2 (1996) (a) specimen 1A, (b) specimen5A

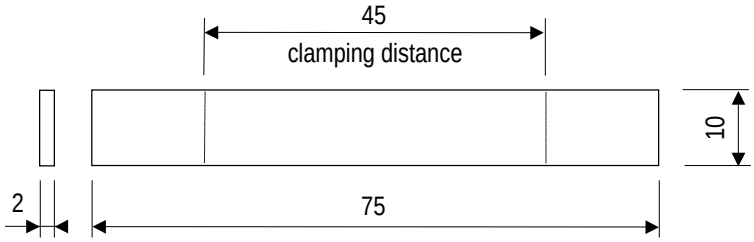

Figure 7 Dimensions of the tensile load-unload-reload test specimen

Tensile load-unload-reload test specimens (as shown in Figure 7) have a rectangular form without reinforcement at the ends. Thus, failure will occur at grips and the strength will be lower than for tensile test specimens but this does not affect the load-unload-reload cycles.

2.2.2 Manufacture

The specimens were made of bulk adhesives and prepared according to the supplier's specifications. After mixing the two components the EP and PU adhesives were poured into a casting mold with adapted dimensions (Figure 8). The ADP adhesive was added in a large plate mould (Figure 9(a)). The specimens were cured under ambient laboratory conditions, 23 ± 1°C and 50 ± 5% relative humidity, for one week. Subsequently, EP and PU specimens were removed from the casting molds and ADP specimens were manufactured by machining the plate to the required dimensions (Figure 9(b)). The specimens were stored under ambient laboratory conditions for four weeks and one week for EP and PU series and ADP series respectively.

Figure 8 Specimen 1A manufactured using a cast mold

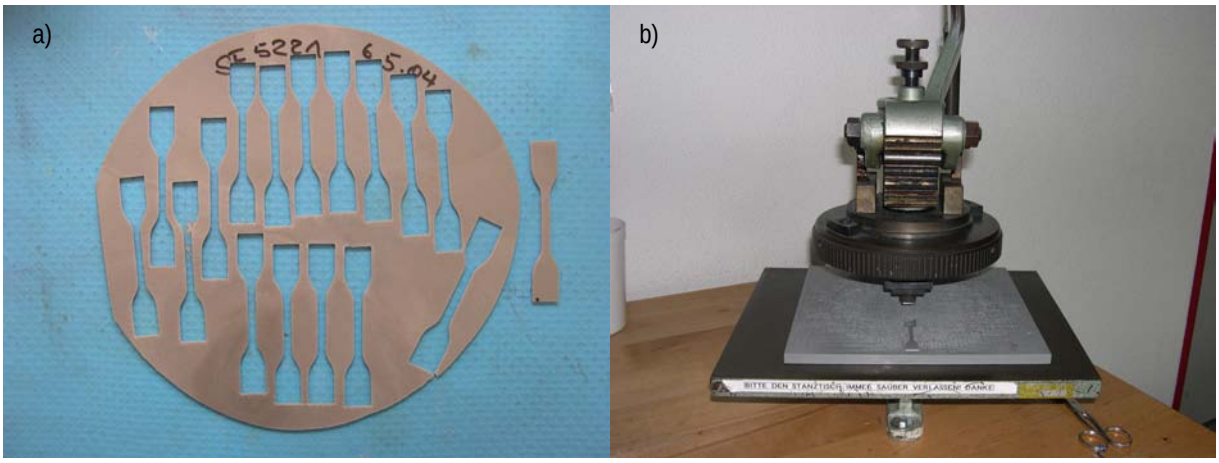

Figure 9 (a) Specimen 5A cut from an adhesive bulk plate; (b) Cutting machine

Air inclusions were observed on the free surfaces of the EP specimens and specially the PU specimens. The second manufacturing technique reduces defects at specimen edges and corners but could also introduce an initial stress state (Jeandrau 1991). It is only used with soft adhesives due to the cutting machine limit.

2.3 Test Procedure

2.3.1 Test Set-Up and Loading Equipment

The specimens were loaded into a tensile testing machine, Zwick Z005, with grips (Figure 10). The fixation procedure induces a prestress load of 3 N in the EP and PU specimens and 1 N in the ADP specimens. The tests were conducted under ambient laboratory conditions, 23 ± 1°C and 50 ± 5% relative humidity. According to EN ISO 527-1 (1996) and the specified specimen geometry (specimen 1A according to EN ISO 527-2 (1996)), the Young's modulus should be determined with a constant displacement rate of 0.5 mm/min and the strength with a constant displacement rate of 5 mm/min. In order to save time and reduce the number of specimens, the Sika laboratory normally changes the testing speed after the Young's modulus has been determined. Thus, the load was applied at two constant displacement rates successively. Tests started at a constant displacement rate of 0.5 mm/min which changed after 0.25% of specimen deformation to 5 mm/min until failure for EP, PU and the first ADP series and to 10/50/100 mm/min for the first, second and third series of ADP specimens. In order to compare adhesive stress-strain curves and because of the adhesive's visco-elastic behavior, the same displacement rate was recommended, that is 5 mm/min until failure. Further evaluation has shown that results for the EP and PU adhesives were not greatly affected by loading rate. The ADP adhesive, however, has a visco-elastic behavior and sensitivity to loading rate.

The load-unload-reload test specimens were loaded into a tensile testing machine, Instron 1185, with grips. Tests began with loading at a displacement rate of 5 mm/min until approximately 50% of specimen strength (approximately 4-5 MPa), then followed the unloading at 1.3 MPa/min, similar to the initial displacement rate, until 0 MPa. The specimens remained unloaded during a period of time (0-5-30 min and 12 hours, one specimen per period). The test finished with a second loading at a displacement rate of 5 mm/min until failure.

2.3.2 Instrumentation and Measurements

The recorded data comprised:

- machine's load cell measurements;
- displacement over the joint's height, measured with the two transducers (Figure 10).

These measurements allow estimation of:

- axial stress, dividing force by cross-section area;

- axial strain, dividing lengthening by initial span of 50 mm;
- tensile Young's modulus.

For all specimens, width and thickness were measured with a micrometer at several points along the span to check tolerances and for axial stress calculation. The specimen thickness contraction used for calculation of transversal strain and determination of the Poisson's ratio could not be measured due to lack of adapted instrumentation.

Concerning the load-unload-reload tensile test, only the load and displacement cell measurements of the machine were recorded.

Figure 10 Tensile testing device

2.4 Test Results and Discussion

2.4.1 Stress-Strain Relationship

Tensile nominal stress-strain curves of the three adhesives are given in Figure 11. These curves are based on the undeformed geometry. The EP demonstrated elastic behavior, almost linear, and brittle failure, while the PU and ADP demonstrated ductile behavior. For a better knowledge of the latter two adhesives, tensile tests with different steps of loading and unloading must be performed in order to determine the corresponding plastic deformations. Only tests on ADP are included in this report.

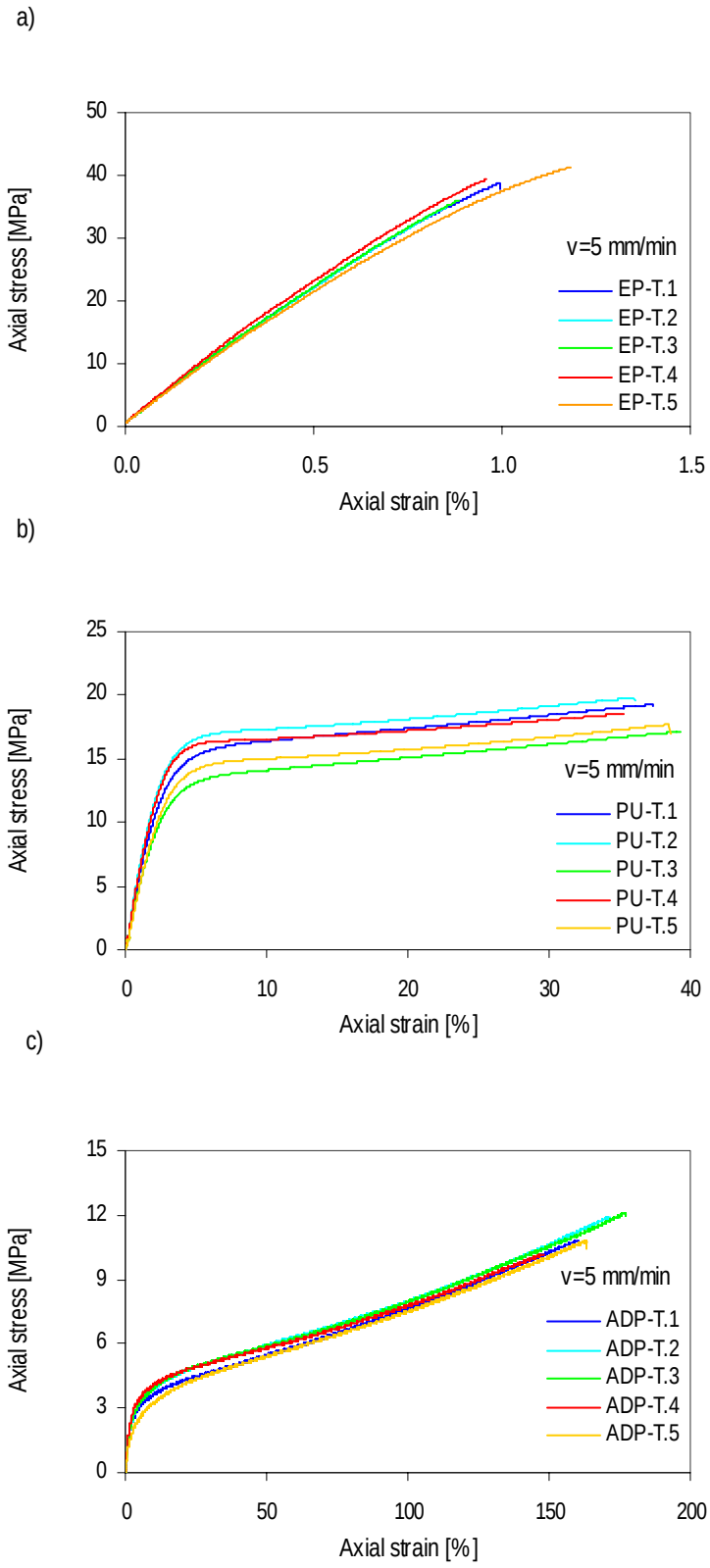

Figure 11 Tensile nominal stress-strain curves for (a) EP, (b) PU, (c) ADP at 5 mm/min

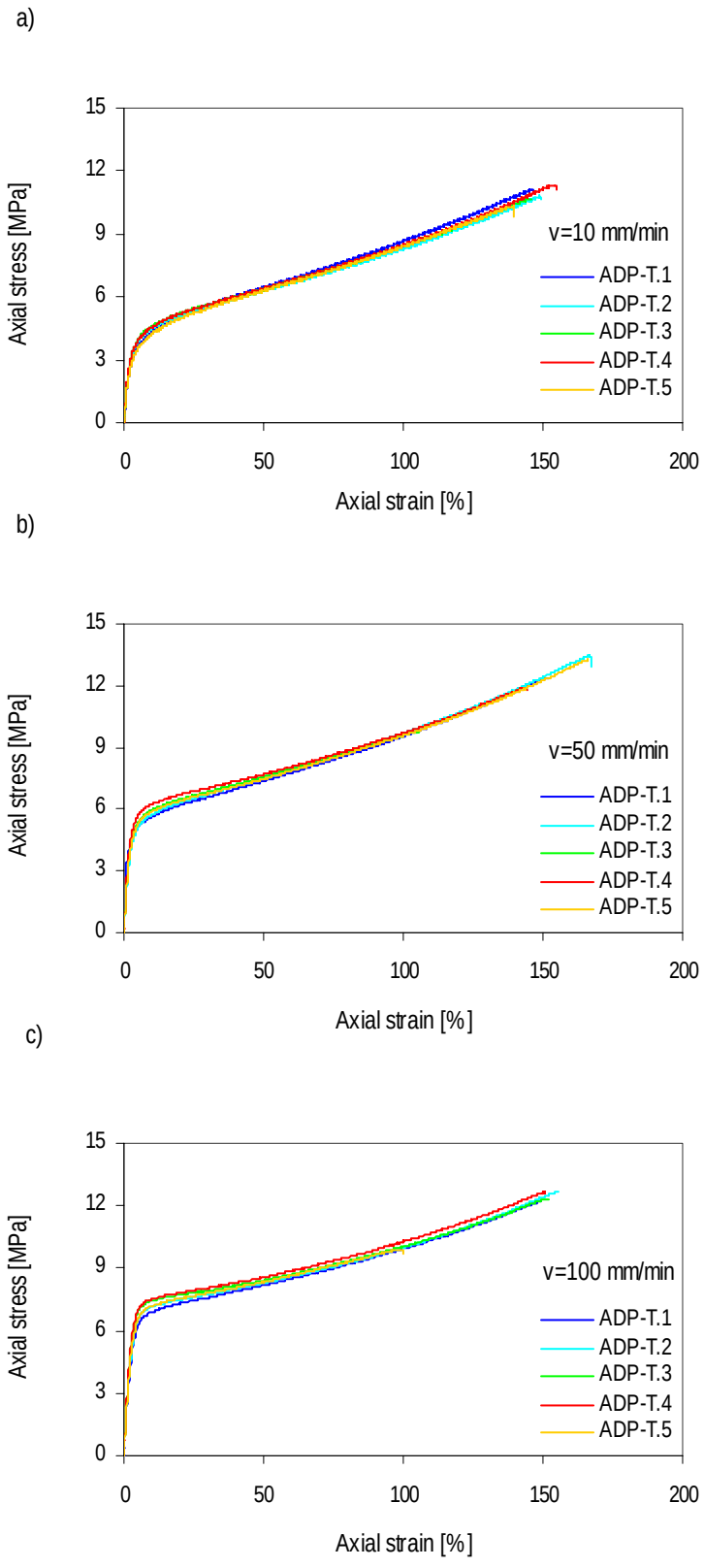

Figure 12 Tensile nominal stress-strain curves for ADP at (a) 10 mm/min, (b) 50 mm/min, (c) 100 mm/min

The EP adhesive set of specimens showed similar uniaxial stress-strain curves (Figure 11(a)). The differences in tensile Young's modulus are not significant but variations in the ultimate tensile stress are large (Table 2). This is probably caused by the amount of voids inside the specimens (see failure modes).

The PU adhesive set of specimens showed similar uniaxial stress-strain curves (Figure 11(b)). The differences in ultimate tensile stress and ultimate tensile strain are not significant but variations in the tensile Young's modulus are large (Table 3).

Both ADP adhesive sets of specimens showed similar uniaxial stress-strain curves (Figures 11(c) and 12(a-c)). Variations in mechanical properties are lower than 10% so results are considered good (Table 4).

Tables 2-7 summarize tensile test results for adhesive properties. They include the tensile ultimate stress, $\sigma_{t,u}$, tensile ultimate strain, $\varepsilon_{t,u}$, and tensile Young's modulus, E_t, of the specimens, the average values and standard deviations. Specimens 3 and 5 were not included in calculation of the latter two values of the ADP series at 50 mm/min and 100 mm/min respectively due to their premature failure. Values of the tensile Young's modulus, E_t, are calculated by taking the secant modulus at the axial strain interval of 0.05-0.25%, which is close to the secant modulus at an axial strain of 0.2% calculated for traditional ductile materials.

Table 2 Tensile test results for EP adhesive properties (5 mm/min)

Specimens	$\sigma_{t,u}$ [MPa]	$\varepsilon_{t,u}$ [%]	E_t [MPa]
EP-T.1	38.8	1.0	4534
EP-T.2	34.9	0.9	4485
EP-T.3	36.0	0.9	4583
EP-T.4	39.4	0.9	4765
EP-T.5	41.3	1.2	4394
m	38.1	1.0	4552
s	2.6	0.1	138

Table 3 Tensile test results for PU adhesive properties (5 mm/min)

Specimens	$\sigma_{t,u}$ [MPa]	$\varepsilon_{t,u}$ [%]	E_t [MPa]
PU-T.1	19.2	1.0	588
PU-T.2	19.7	0.9	641
PU-T.3	17.1	0.9	500
PU-T.4	18.5	0.9	614
PU-T.5	17.7	1.2	510
m	18.4	37.1	571
s	1.0	1.5	56

Table 4 Tensile test results for ADP adhesive properties (5 mm/min)

Specimens	$\sigma_{t,u}$ [MPa]	$\varepsilon_{t,u}$ [%]	E_t [MPa]
ADP-T.1	10.8	160.2	204
ADP-T.2	11.9	171.8	216
ADP-T.3	11.8	177.0	211
ADP-T.4	10.2	148.0	229
ADP-T.5	10.8	163.5	181
m	11.1	164.1	208
s	0.7	11.2	18

Table 5 Tensile test results for ADP adhesive properties (10 mm/min)

Specimens	$\sigma_{t,u}$ [MPa]	$\varepsilon_{t,u}$ [%]	E_t [MPa]
ADP-T.1	11.1	146.5	259
ADP-T.2	10.8	149.1	270
ADP-T.3	10.7	145.9	275
ADP-T.4	11.3	154.7	267
ADP-T.5	10.3	139.8	247
m	10.9	147.2	264
s	0.4	4.8	10

Table 6 Tensile test results for ADP adhesive properties (50 mm/min)

Specimens	$\sigma_{t,u}$ [MPa]	$\varepsilon_{t,u}$ [%]	E_t [MPa]
ADP-T.1	12.4	152.9	283
ADP-T.2	13.5	167.2	299
ADP-T.3	9.8	105.4	321
ADP-T.4	11.9	144.1	320
ADP-T.5	13.3	166.3	289
m	12.8	157.6	298
s	0.8	0.8	16

Table 7 Tensile test results for ADP adhesive properties (100 mm/min)

Specimens	$\sigma_{t,u}$ [MPa]	$\varepsilon_{t,u}$ [%]	E_t [MPa]
ADP-T.1	12.2	148.7	287
ADP-T.2	12.7	155.3	284
ADP-T.3	12.3	151.9	355
ADP-T.4	12.6	151.0	353
ADP-T.5	9.9	99.9	298
m	12.5	151.7	320
s	0.2	2.7	40

Tensile nominal stress-strain curves of ADP specimens loading-unloading-reloading at 5mm/min are illustrated in Figure 13(a). These curves are based on the undeformed geometry. Specimens exhibited a premature failure compared with specimens just loaded in tension up to failure (Figure 11(c)) since failure occurred at grip areas. Nevertheless, curves shapes are similar. The loading and unloading behaviors were different due to adhesive visco-elasticity while loading and reloading behaviors were similar. The recreep strain (during the recovering period, at 0 MPa) increased with recovering period. Figure 13(b) illustrated the time-dependent recreep strain to instantaneous strain (just after unloading) ratio. The ratio higher increase occurred within the first 30 min. An extended experimental investigation on this field should be carried out leading to conclusions.

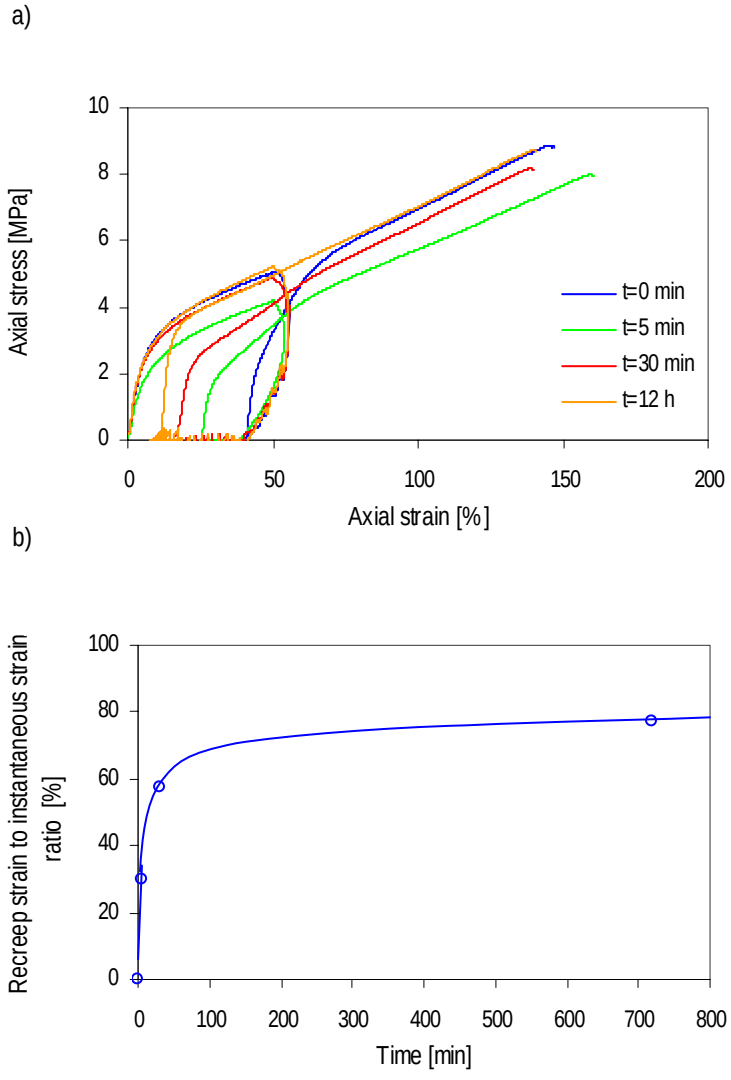

Figure 13 (a) Tensile load-unload-reload nominal stress-strain curves for ADP (5 mm/min); (b) Time-dependent recreep strain to instantaneous strain ratio

2.4.2 Failure Modes

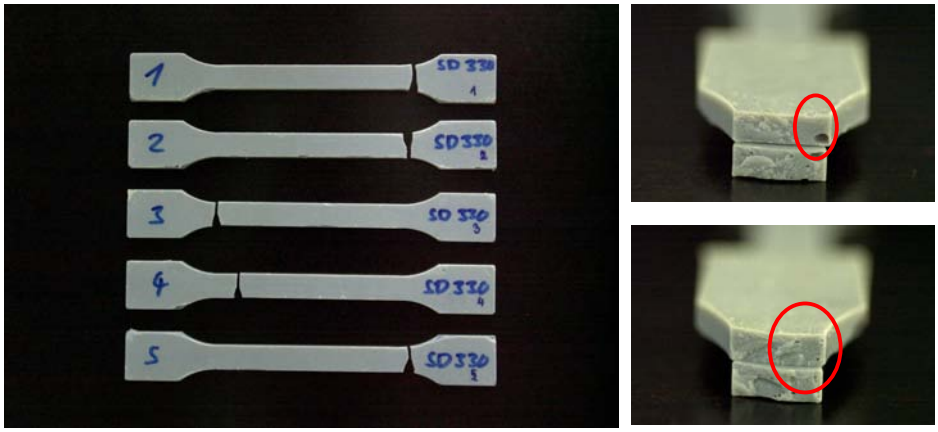

Figure 14 EP (a) tensile specimens after failure; fracture surfaces (b) EP-T.1, (c) EP-T.5

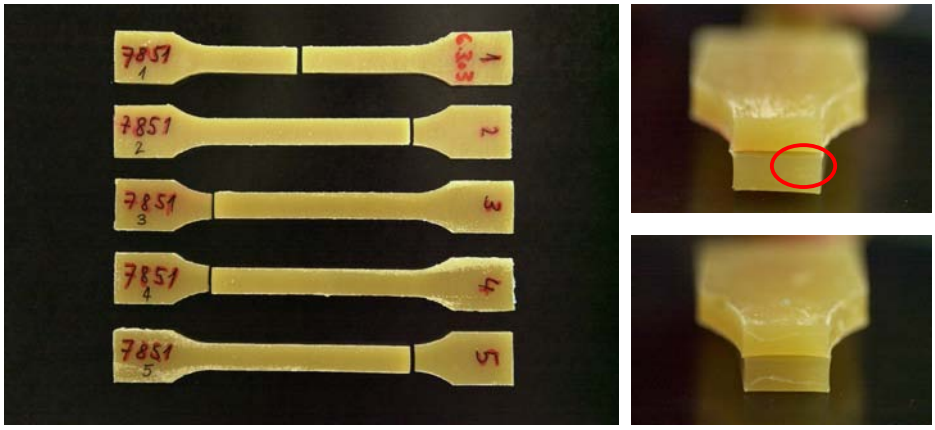

Figure 15 PU (a) tensile specimens after failure; fracture surfaces (b) PU-T.1, (c) PU-T.5

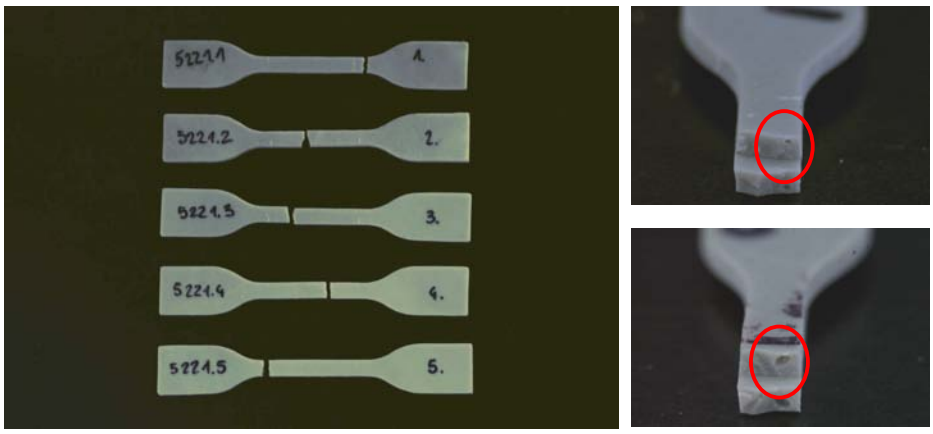

Figure 16 ADP (a) tensile specimens after failure; fracture surfaces (b) ADP-T.3, (c) ADP-T.4 (5 mm/min)

With the exception of specimen 4, failure of EP specimens occurred in the curve area (Figure 14(a)). This area probably had more voids than the central part of the specimens because of the curvature. All specimen fracture surfaces exhibit small voids. On the fracture surfaces of specimens 1, 2 and 3, the voids are of considerable size: up to 2 mm, whereas in 4 and 5, the voids are smaller than 0.5 mm (Figures 14(b) and (c)). This could explain why the strength of these two specimens was greater than that of the others. Voids have the same effect as micro-cracks; they produce stress concentration and cause fracture of the specimen. Since the EP set of specimens was the first series manufactured and tested, specimen quality was the worst of all the series.

With the exception of specimen 1, failure of PU specimens occurred in the curve area as for EP specimens (Figure 15(a)). Specimen 1 had a 0.8 mm wide void on the bottom free surface whereas no voids were observed in other specimens (Figures 15(b) and (c)). This probably explains the different failure location on this specimen compared to the others. Specimens 1 and 2 were lighter than the others, but this does not seem to have influenced test results. There is as yet no explanation for this color difference.

ADP specimens (v=5 mm/min) 1 and 5 failed in the curve area, whereas ADP specimens 2, 3 and 4 failed in the span (Figure 16(a)). No voids were observed in specimens 1, 2 and 5. Specimens 3 and 4 had 0.2 mm and 1.0 mm wide voids respectively (Figures 16(b) and (c)). The large void in specimen 4 may explain its lower failure load compared to the others.

2.4.3 Summary

The nominal stress-strain curves are based on undeformed geometry. While adhesives, especially PU and ADP, exhibited large deformations, since length and cross-section during the test differed significantly from the initial ones, instantaneous dimensions must be considered. Thus, the nominal stress and nominal strain must be transformed into the true stress and strain. If it is assumed that specimen volume does not change, the true stress and true strain are respectively equal to:

$$\sigma_{t,\tau} = \sigma_\tau \frac{L}{L_o} = \sigma_\tau (1+\varepsilon_\tau) \tag{1}$$

$$\varepsilon_{t,\tau} = \int_{L_0}^{L} \frac{1}{L} dL = \ln(\frac{L}{L_0}) = \ln(1+\varepsilon_\tau) \tag{2}$$

where L_o is initial measurement length, L is measurement length at any time and dL is the increment of elongation relative to the measurement length of L. The average nominal stress-strain curves were determined for each adhesive and displacement rate. Then the true average stress-strain curves were deduced. Figure 17(a) shows the behavior of the EP, PU and ADP series loaded at the 5, 10, 50 and 100 mm/min displacement rates and Figure 17(b) focuses on the ADP series.

The ADP adhesive exhibited visco-elastoplastic behavior as observed comparing the four series loaded at different displacement rates (Figure 17(b)). In general, higher strength and lower failure strain are expected when testing at higher displacement rates (Hart-Smith 1990) but this was not observed in

the test since failure strain increased slightly with the high rate. This probably indicates better specimen quality.

The EP adhesive is modeled with linear behavior and the PU and ADP adhesives are modeled with bilinear behavior. The EP linear model is characterized by the tensile elastic modulus, $E_{t,e}$, at the axial strain interval of 0.5-1%, the tensile ultimate stress, $f_{t,u}$, and the tensile ultimate strain, $\varepsilon_{t,u}$. The PU and ADP bilinear models are characterized by the tensile elastic modulus, $E_{t,e}$, the tensile plastic modulus, $E_{t,p}$, the tensile elastic stress, $f_{t,e}$, the tensile ultimate stress, $f_{t,u}$, and the tensile ultimate strain, $\varepsilon_{t,u}$ (Figure 18). The elastic modulus $E_{t,e}$ is defined at the axial strain interval of 0.5-1% and $E_{t,p}$ at the axial strain interval of 10-20% for PU and 30-50% for ADP adhesive. Table 5 summarized the tensile mechanical properties for the adhesive models. Figure 19 shows the tensile model stress-strain curves for the three adhesives.

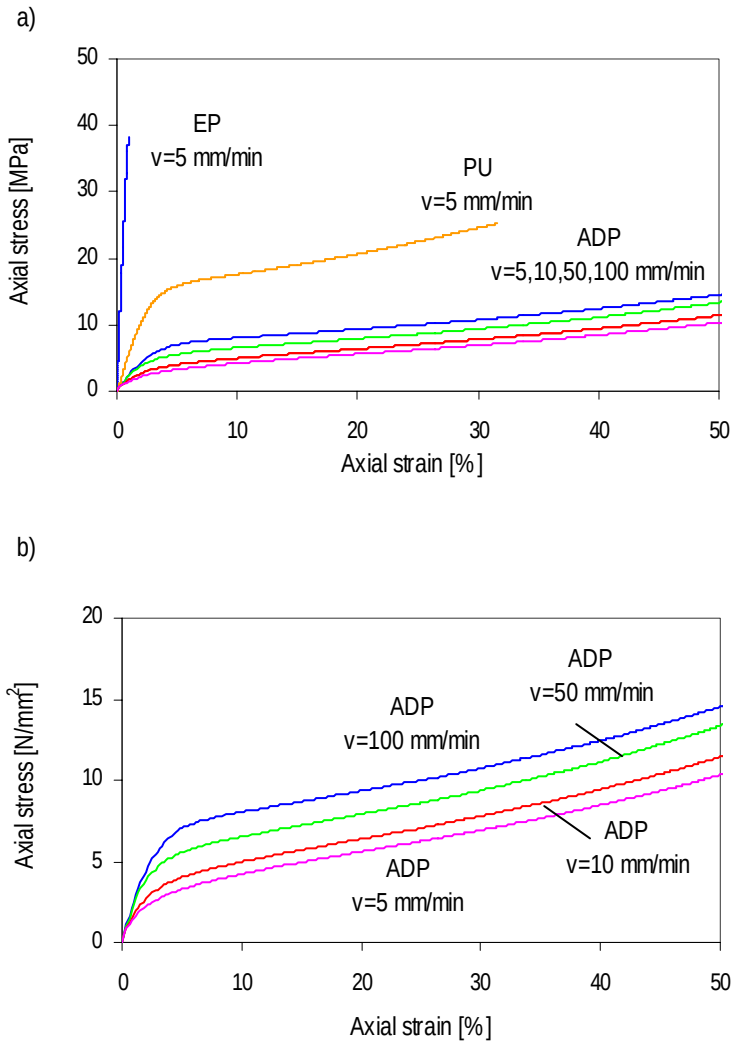

Figure 17 Average true tensile stress-strain curves for (a) EP, PU (v=5 mm/min) and ADP (v=5,10,50,100 mm/min), (b) ADP loaded at four displacement rates: 5, 10, 50 and 100 mm/min

As previously noted, specimen thickness contraction, necessary for determination of the Poisson's ratio, could not be measured due to lack of appropriate instrumentation. Schmid (2002) gives indications for this value. He considered the EP and PU adhesive Poisson's ratios were 0.37 and 0.42 respectively. The ADP adhesive Poisson's ratio is assumed to be 0.40 (between EP and PU adhesives (Venetz 2004)).

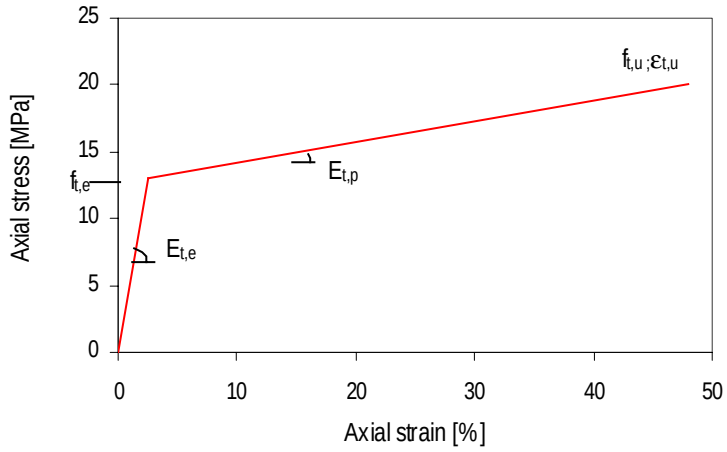

Figure 18 Tensile model stress-strain curves for PU and ADP

Table 8 Tensile mechanical characteristics of adhesive models

Adhesive	$f_{t,u}$ [MPa]	$\varepsilon_{t,u}$ [%]	$E_{t,e}$ [MPa]	$E_{t,p}$ [MPa]	$f_{t,e}$ [MPa]	ν [-]
EP[1]	39	1	4563	-	-	0.37
PU[1]	25	32	586	31	15	0.42
ADP[1]	29	97	101	14	3	0.40
[2]	27	91	136	14	4	
[3]	31	93	216	14	5	
[4]	30	91	230	15	7	

load applied with a displacement rate of [1] 5 mm/min, [2] 10 mm/min, [3] 50 mm/min, [4] 100 mm/min

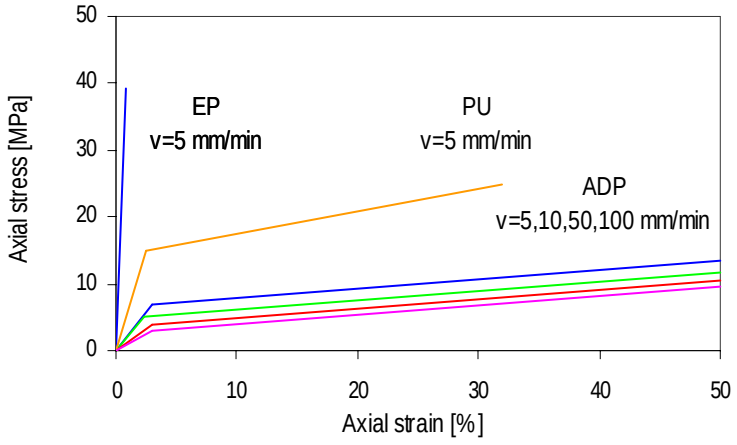

Figure 19 Tensile model stress-strain curves for EP, PU and ADP

3 Compression Tests

3.1 Compression Test Choice

The comments made concerning tensile test choice also apply to the compression tests. Bulk specimens are preferred to butt joints. The bulk compression specimens may be cylindrical, parallelepiped (square or rectangular base) or tubular. The adhesive bulk tests provide stress-strain curves and therefore compressive Young's modulus, elastic limit and failure characteristics.

3.2 Test Specimen

3.2.1 Dimensions

For each of the three adhesives, five compressive test specimens were used (as shown in Figure 20). For the PU and ADP adhesives, only four specimens were prepared and tested because the request did not reach the Sika laboratory. Despite this and because test results were consistent, no additional specimens were tested.

Specimens had a parallelepiped form with a square section according to ASTM D 695-96.

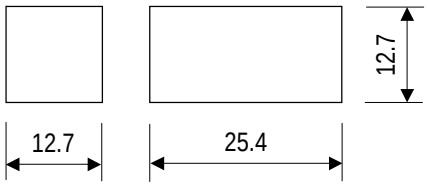

Figure 20 Dimensions of the compression test specimen according to ASTM D 695-96 (1996)

3.2.2 Manufacture

The specimens were made from bulk adhesives and prepared according to the supplier's specifications in the same way as the tensile test specimens.

Air inclusions were observed on the free surface of the EP and PU specimens (Figures 23 and 24, page 27). The EP specimens had some imperfections at the corners and the PU specimens at the edges (Figure 23).

3.3 Test Procedure

3.3.1 Test Set-Up and Loading Equipment

The specimens were loaded into a compression testing machine, Instron 5500R 1185, which was formed by two plates. The bottom plate was fixed and the top plate mobile (Figure 21). The tests were conducted under ambient laboratory conditions, 23 ± 1°C and 50 ± 5% relative humidity. The load was applied at a constant displacement rate of 1.3 mm/min up to a nominal strain of 5% for the EP,

60% for the PU and for the ADP adhesives according to ASTM D 695-96 (1996). Different maximum strains were designated for each adhesive because of their very different stiffness and deformability.

3.3.2 Instrumentation and Measurements

The recorded data comprised:

- machine's load cell measurements;
- displacement of mobile plate.

These measurements allow estimation of:

- axial stress, dividing force by cross-section area;
- axial strain, dividing change in length by initial height;
- compressive Young's modulus.

For all specimens, both sides of the square section and the height were measured with a micrometer at several points to check tolerances and for axial stress calculation.

Figure 21 Compression testing device

3.4 Test Results and Discussion

3.4.1 Stress-Strain Relationship

Compressive nominal stress-strain curves for the three adhesives are given in Figure 22. These curves are based on the undeformed geometry.

The EP adhesive set of specimens showed similar uniaxial stress-strain curves (Figure 22(a)). The specimens exhibited linear behavior up to approximately 60% of maximum compressive strain. Variations in mechanical properties were not significant (Table 6).

The PU adhesive set of specimens showed similar uniaxial stress-strain curves (Figure 22(b)). Variations in the compressive Young's modulus were large (Table 7). This was probably caused by the amount of voids inside the specimens (see failure modes).

The ADP adhesive set of specimens showed similar uniaxial stress-strain curves (Figure 22(c)). Variations in the compressive Young's modulus were large (Table 8). As in the case of the tensile specimens, no differences were detected in the compressive specimens that could explain these variations. Therefore the test results are considered valid.

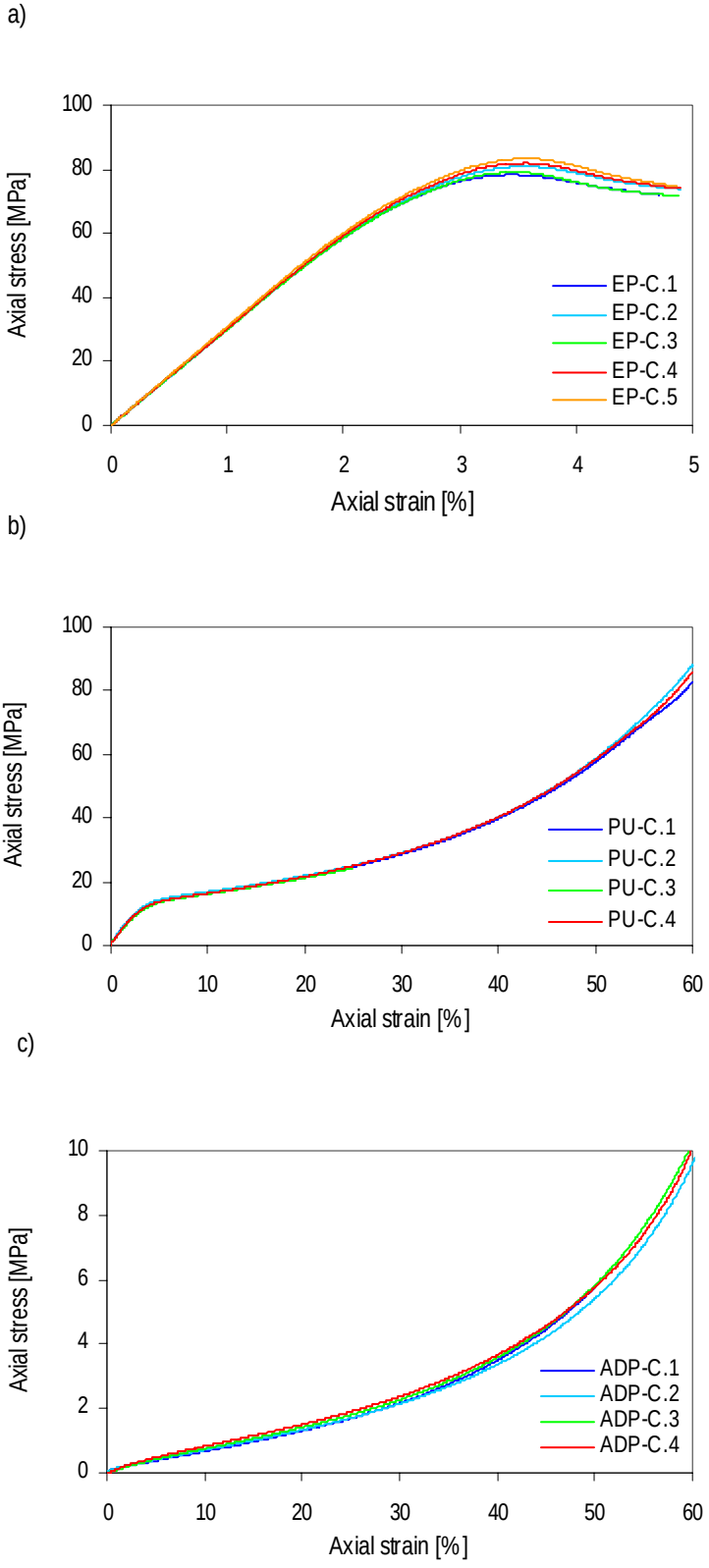

Figure 22 Compressive nominal stress-strain curves for (a) EP, (b) PU, (c) ADP

Tables 6, 7 and 8 summarize compression test results for adhesive properties. Table 6 includes the compressive maximum stress, $\sigma_{c,max}$, respective compressive strain, $\varepsilon_{c,max}$, compressive Young's modulus, E_c, of the specimens, the average values and standard deviations. The compressive maximum stress corresponded to the strength of the EP specimens and maximum measured value of the PU and ADP adhesives (related to the maximum strain $\varepsilon_{c,max}$=60%). Specimen 3 of the PU series was not included in the average and standard deviation calculation of maximum compressive stress due to the specimen's irregular behavior as from ε_c =30%. Specimen 1 of the ADP series was not included in the average and standard deviation calculation of the maximum compressive stress due to the premature stopping of loading. The values of compressive Young's modulus, E_c, are calculated by taking the secant modulus at an axial strain interval of 0.05-0.25%.

Table 9 Compression test results for EP adhesive properties (1.3 mm/min)

Specimens	$\sigma_{c,u}$ [MPa]	$\varepsilon_{c,u}$ [%]	E_c [MPa]
EP-C.1	78.3	3.4	3042
EP-C.2	80.9	3.6	3030
EP-C.3	79.0	3.4	3019
EP-C.4	81.9	3.6	3055
EP-C.5	83.3	3.6	3105
m	80.7	3.5	3050
s	2.1	0.1	33

Table 10 Compression test results for PU adhesive properties (1.3 mm/min)

Specimens	$\sigma_{c,u}$ [MPa]	$\varepsilon_{c,u}$ [%]	E_c [MPa]
PU-C.1	82.9	60	415
PU-C.2	87.9	60	385
PU-C.3	27.9	30	347
PU-C.4	86.0	60	335
m	85.6	60	371
s	2.5	0	37

Table 11 Compression test results for ADP adhesive properties (1.3 mm/min)

Specimens	$\sigma_{c,u}$ [MPa]	$\varepsilon_{c,u}$ [%]	E_c [MPa]
ADP-C.1	5.8	50	8
ADP-C.2	9.6	60	10
ADP-C.3	10.3	60	8
ADP-C.4	10.0	60	12
m	10.0	60	9
s	0.4	0	2

3.4.2 Failure Modes

EP specimen failure occurred along a surface inclined at α= 40-45° to the vertical axis (Figure 23). This is the typical failure mode of stiff and brittle materials such as stone, brick or cast iron.

PU and ADP specimen failure is difficult to analyze since the specimens were compressed to high levels, up to a contraction of 60% and 80% respectively (Figures 24 and 25). This is especially true for the ADP specimens.

The PU specimens exhibited a kind of buckling failure (Figure 24). Specimens 3 had an internal light area incline at α= 30° to the vertical axis that could be a failure surface.

In the ADP specimens, the large longitudinal contraction induced high transversal deformations. Due to a high Poisson's ratio, this produced a transversal expansion of the specimens and internal failure. Thus, this study considers only measurements up to 60 % of the compressive strain.

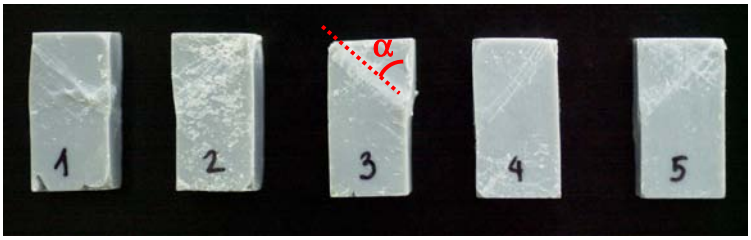

*Figure 23 EP compression specimens after failur*e

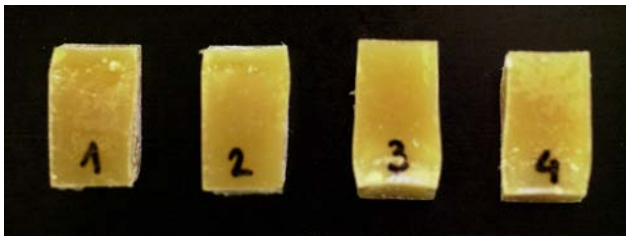

Figure 24 PU compression specimens after « failure »

Figure 25 ADP compression specimens after failure

3.4.3 Summary

The nominal stress-strain curves are based on undeformed geometry. With regard to tensile tests, the adhesives exhibited large deformations. Thus, the nominal stress and nominal strain must be corrected to the true stress-strain curves (see 3.3.3).

The average nominal stress-strain curves were determined for each adhesive. Then the true average stress-strain curves were deduced. Figure 26 shows the average true stress-strain curves and the model stress-strain curves of the EP, PU and ADP series in compression.

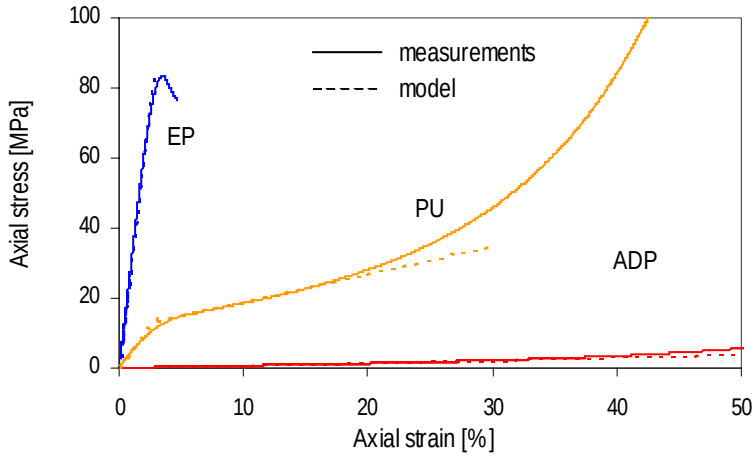

Figure 26 Average true compressive stress-strain curves for EP, PU and ADP adhesives, measurements and models

The adhesives EP and ADP are modeled with linear behavior and the adhesive PU is modeled with bilinear behavior. The EP linear model is characterized by the compressive elastic modulus, $E_{c,e}$, at the axial strain interval of 0.5-1%, maximum compressive stress, $f_{c,u}$, and maximum compressive strain, $\varepsilon_{c,u}$. The PU bilinear model is characterized by the compressive elastic modulus, $E_{c,e}$, the compressive plastic modulus, $E_{c,2}$, and the compressive elastic stress, $f_{c,e}$, (see Figure 18). The elastic modulus $E_{c,e}$ is defined at the axial strain interval of 0.5-1% and the plastic modulus $E_{c,p}$ at the axial strain interval of 10-20%. The ADP linear model is only characterized by the compressive elastic modulus, $E_{c,e}$, at the axial strain interval of 0.5-1%. Table 12 summarizes the compressive mechanical properties for the adhesive models.

Table 12 Compressive mechanical characteristics of adhesive models

Adhesive	f_{cu} [MPa]	$\varepsilon_{c,u}$ [%]	$E_{c,e}$ [MPa]	$E_{c,p}$ [MPa]	f_{ce} [MPa]
EP	84	3	3064	-	-
PU	-	60	433	79	13
ADP	-	60	10	-	-

4 Shear Tests

4.1 Shear Test Method Choice

The test specimen most commonly used by manufacturers is the single-lap joint primarily because many joints have this geometrical configuration and it seems to replicate actual conditions, but also because it is simple and economical (Figure 27(a)). However, the joint is misaligned in such a way that under load, it bends and creates a complex stress situation characterized by through-thickness stresses and non-uniform shear stress distribution. Thus, the single-lap joint has a big disadvantage in that results depend on joint characteristics, geometry and surface preparation, rather than solely on intrinsic adhesive properties. It can, however, be used for comparison studies under the same conditions. Cognard (2000) considered the lap joint as a construction method and not as a test method because it is influenced by all bonding parameters.

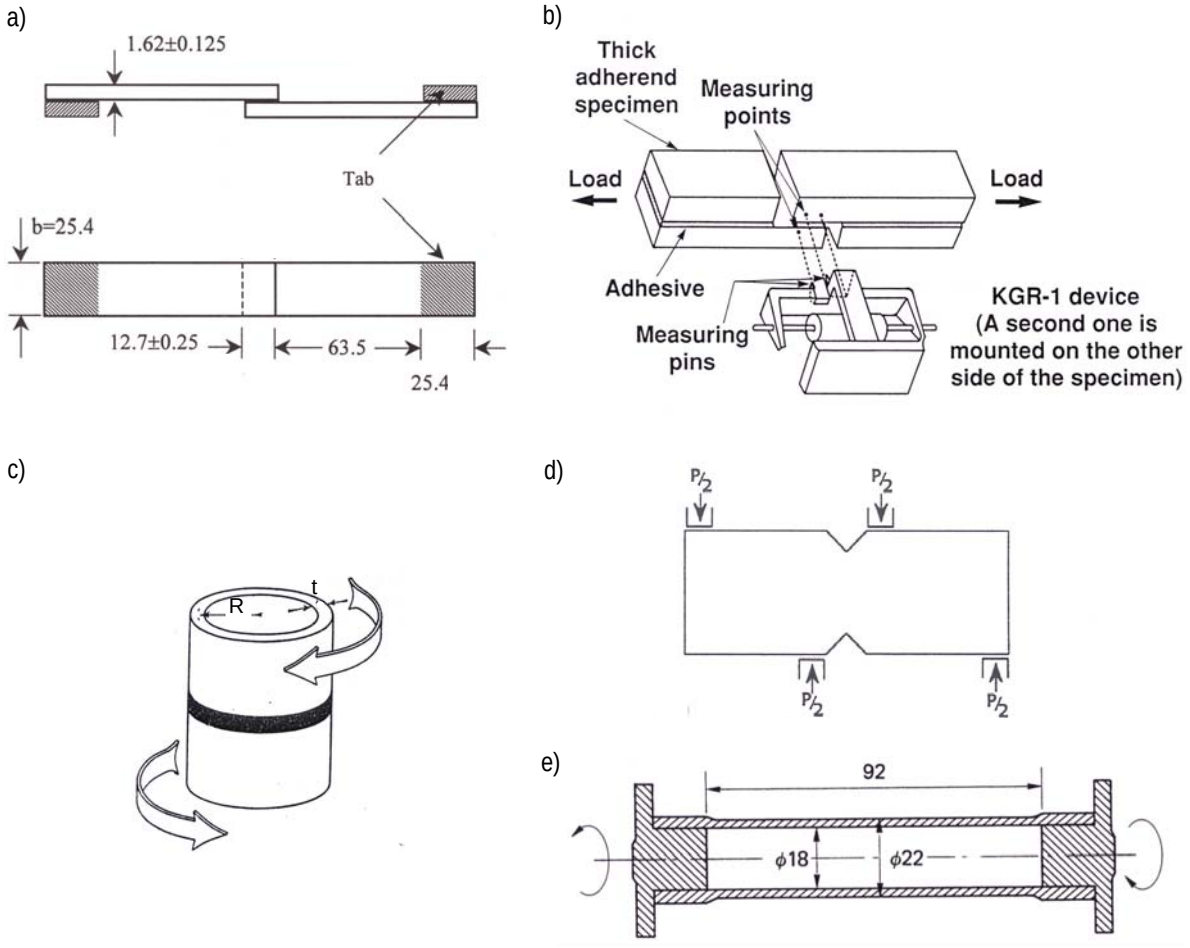

Figure 27 (a) Single-lap joint specimen according to ASTM D 1002 (1999); (b) KGR-1 measuring device and thick adherend shear specimen (Kassapolou and Adelmann 1991); (c) Shear butt joint specimen (De Bruyne 1951); (d) Iosipescu specimen (Adams et al. 1997); (e) Bulk shear specimen (Jeandrau 1991)

The thick adherend shear test has a simple joint geometry, and is thus easy to manufacture and economical (Figure 27(b)). The thick adherends are used in order to minimize bending effects and non-uniform strains. Nevertheless, Kassapolous and Adelmann (1991) have shown that specimen geometry and materials give a non-uniform shear strain distribution for some adhesive thicknesses and stiffnesses. Thus, the ASTM D 3983-98 thick adherend shear test method is suitable for joints with stiff adherends and flexible adhesives. The ratio of the adherend tensile modulus to the adhesive shear modulus should be higher than 300 and adhesive shear modulus should be lower than 700 MPa.

The Iosipescu test can either be in bulk form or as a joint between thick and stiff adherends (Figure 27(d)) (Adams et al. 1997). As for the previous test, the apparently uniform shear stress state was achieved and a major stress concentration developed at the ends.

The butt joint loaded in torsion, called the "napkin-ring" test, ensures a pure state of shear stress in the adhesive layer if the two tubes are perfectly aligned (Figure 27(c)). De Bruyne (1951) suggested that the butt joint specimen should take the form of two thin-walled cylinders ("napkin-rings") bonded together to reduce the variation of shear stress across the adhesive. Specimen production is expensive and difficult, but the main problem is the complexity of the required equipment - the apparatus to generate the torsion and the means of measuring the rotation. In the napkin-ring and the thick adherend shear tests, adhesive shear strains are calculated taking in account deformations in the adherends.

The adhesive shear bulk test, developed by Dolev and Ishai (1981), is a tubular specimen of bulk adhesive tested under torsion (Figure 27(e)). No standard exists for this type of test.

The napkin-ring test is preferred to the other tests in this project, as it provides shear stress-strain curve and therefore shear modulus, elastic limit and failure characteristics.

4.2 Test Specimen

4.2.1 Dimensions

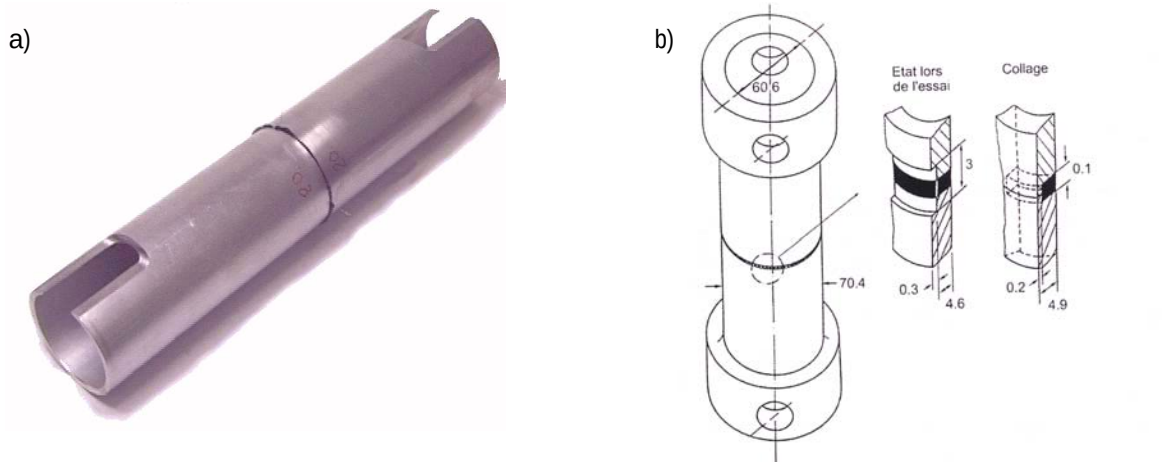

Figure 28 (a) Napkin-ring specimen; the spacer (Schmid and Kieselbach 2003); (b) controlling bondline thickness during curing is removed with a lathe before the test (from Bassetti 2001)

For the three adhesives, four napkin-ring specimens in accordance with Figure 28(a) were prepared and tested. Specimens take the form of two thin-walled cylinders bonded together, designed to improve the weaker features of the former standard EN ISO 11003-1. The cylinders have a 50 mm diameter and 3 mm thickness and are made of an AA6082 aluminum alloy. The bondline thickness is 0.1 mm.

4.2.2 Manufacture

Before bonding, the surfaces of the adherends were sanded and degreased. The adhesives were prepared according to the supplier's specifications. After mixing the two adhesive components, the uncured adhesive was applied to the bottom cylinder (Figures 29(a) and (b)). The cylinders were then bonded. The specimens were stored in a support and cured under ambient laboratory conditions, 23 ± 1°C and 50 ± 5%, for one week (Figures 29(c) and (d)).

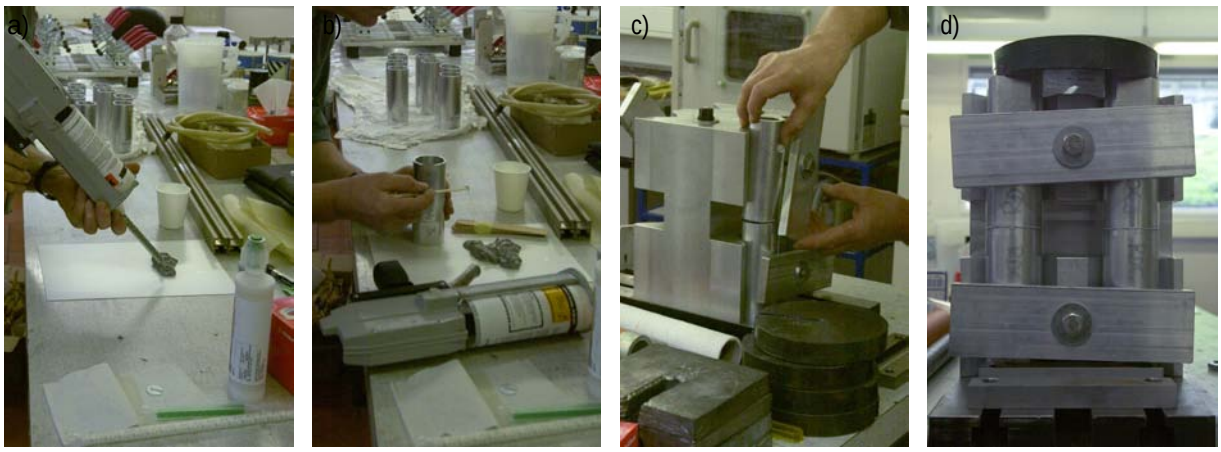

Figure 29 Specimen manufacture: (a) adhesive preparation; (b) adhesive applied to bottom cylinder; (c) cylinder bonding; (d) specimen cure

Fischer and Pasquier (1989) suggested controlling the thickness of the bondline by a 0.1mm rim along the outer perimeter of the upper adherend (Figure 28(b)). Before testing, the rim is removed with a lathe. Deuring (1993) and Bassetti (2001) also used this method. The turning process certainly has a negative influence on parameters tested, but any kind of spacer element has some influence on the bondline, thus the 0.1 mm rim was adopted for the tested specimens.

4.3 Test Procedure

4.3.1 Test Set-Up and Loading Equipment

The specimens were twisted in a testing machine with grips (Figure 30(a)). The tests were conducted under ambient laboratory conditions, 23 ± 1°C and 50 ± 5%. The load was applied at a constant displacement rate to produce specimen failure in approximately 1 min.

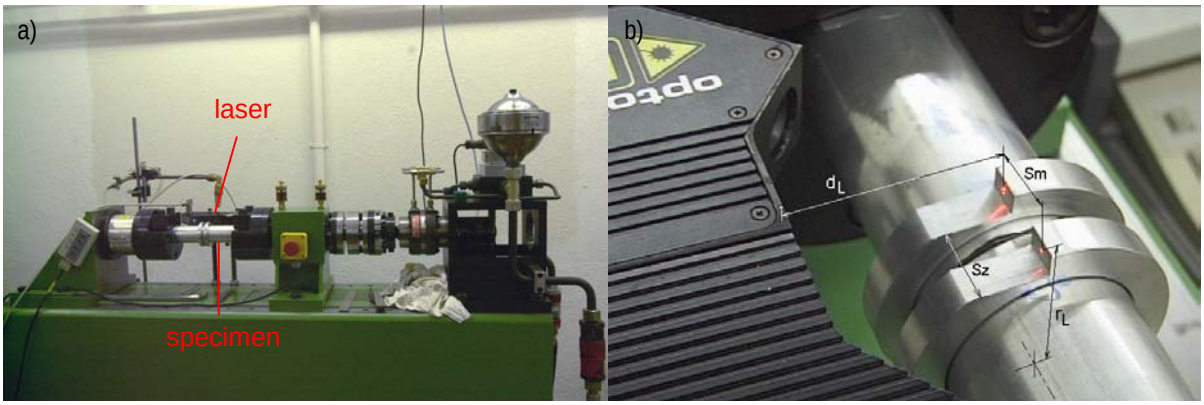

Figure 30 (a) Shear testing device; (b) Laser triangulation (EMPA Dübendorf)

4.3.2 Instrumentation and Measurements

The recorded data comprises:

- the machine's torque cell measurements, T;
- displacement between two points on each adherend, v_m, measured with a laser (Figures 25 and 30(b)).

This displacement, v_m, consists of displacement of the adhesive, v_a, and displacement caused by twisting of the adherends, v_t. These measurements allow estimation of:

- shear stress;
- shear strain;
- shear modulus.

The applied torque T can be expressed as (see Figure 31(b)):

$$T = \int_A r dA = \int_{r_i}^{r_o}\int_0^{2\pi} r^2 \tau(r) dr d\phi = \frac{\pi}{2}\cdot\frac{\tau_o}{r_o}\cdot(r_o^4 - r_i^4) \tag{3}$$

with shear distribution along the tube thickness: $\tau(r) = \frac{\tau_o}{r_o}\cdot r$ (4)

Shear stress in the medium radius is determined with: $r = \frac{r_i + r_o}{2}$:

$$\tau = \frac{T}{\pi}\cdot\frac{1}{(r_o^2 + r_i^2)(r_o - r_i)} \tag{5}$$

Shear strain is:

$$\gamma = \frac{v_a}{d} = \frac{v_m - v_t}{d} \tag{6}$$

where v_t is calculed from the shear stress in the adherends and the known shear modulus of aluminum.

And shear modulus is given by:

$$G = \frac{\tau}{\gamma} \text{ (from the linear part of the stress-strain curve)} \quad (7)$$

For the specimen dimensions (r_i=44 mm, r_o=50 mm), the difference between shear stress in the outer and medium radii is 6%. Thus, it is negligible.

T	:	torque	v_m	:	displacement measured in the specimen
r_i	:	inner radius	v_a	:	displacement of the adhesive
r_o	:	outer radius	v_t	:	displacement caused by the twist of the adherends
γ	:	shear strain	d	:	adhesive thickness

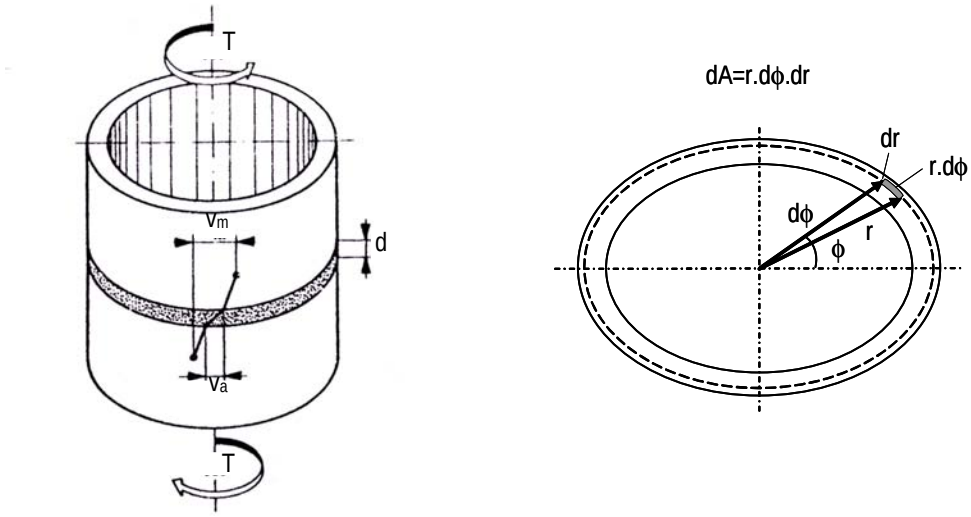

Figure 31 (a) Displacements on surface of bonded cylinders (Fischer and Pasquier (1989)); (b) Area parameters for torque calculation

4.4 Test Results and Discussion

4.4.1 Shear Stress-Strain Relationship

EMPA evaluated the recorded data and supplied shear stress-strain curves for the three adhesives. Unfortunately, EP specimen measurements were not useful (Figure 32(a)). Furthermore, the EP is certainly too stiff to be tested using this kind of specimen developed for soft adhesives. Only two of the four PU and ADP specimens prepared and tested gave similar results.

The PU adhesive specimens exhibited different shear stress-strain curves but with the same tendency (Figure 32(b)). The differences in mechanical properties were not significant (Table 10).

The ADP adhesive specimens exhibited similar shear stress-strain curves (Figure 32(c)). The shear moduli were identical and the ultimate shear stress and shear strain were similar (Table 10).

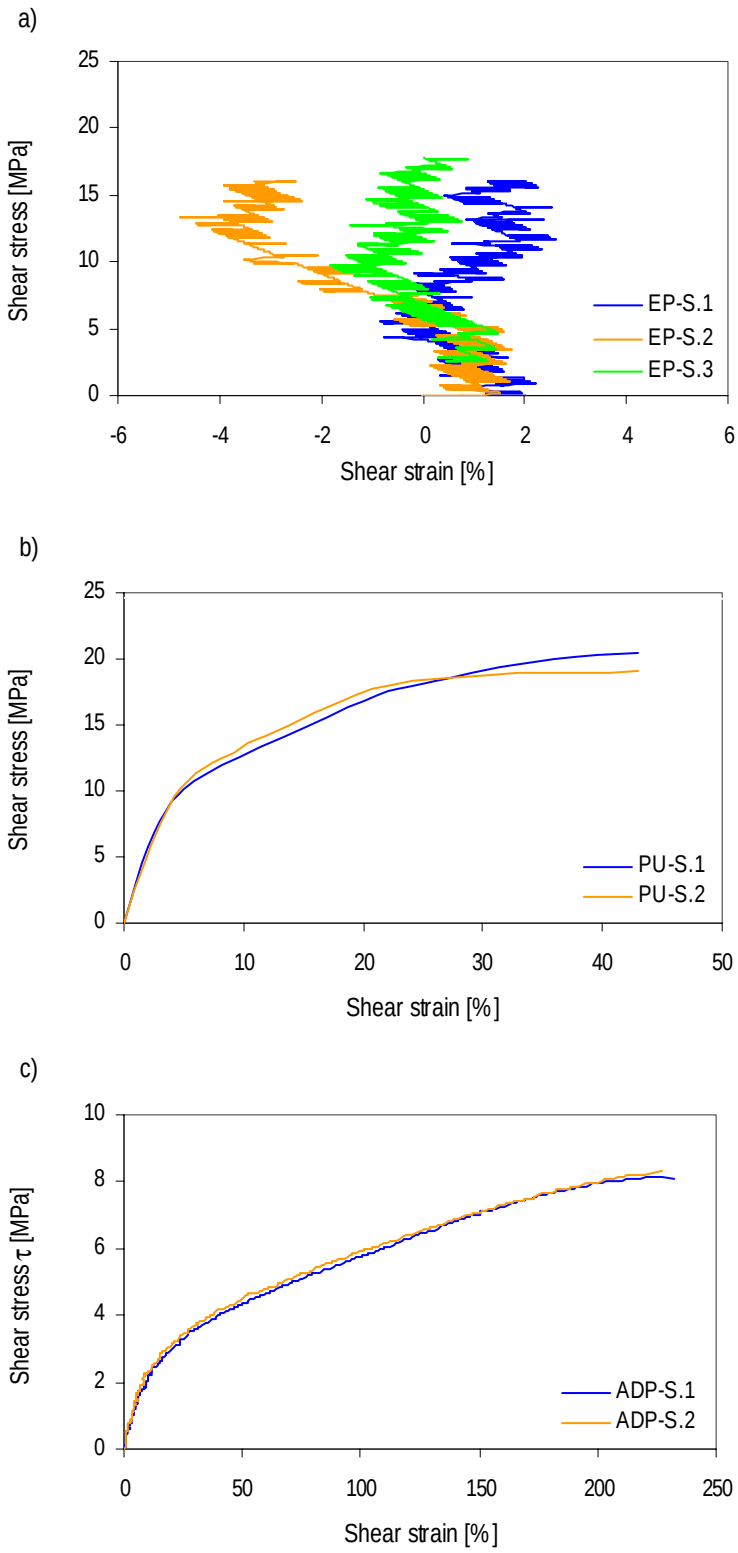

Figure 32 Shear nominal stress-strain curves for (a) EP, (b) PU, (c) ADP

4.4.2 Failure Modes

Failure of EP and PU specimens occurred in the interface between the adhesive layer and adherends indicating adhesion problems between these two materials (Figures 34 and 35). The failure of ADP specimens was a combination of failure in the adhesive layer and in the interface (Figure 35).

4.4.3 Summary

The PU and ADP adhesives are modeled with bilinear shear behavior characterized by the shear elastic and plastic moduli, G_e and G_p, the shear elastic stress, τ_e, the shear ultimate stress, τ_u, and the shear ultimate strain, γ_u, of the specimens. Values of the shear elastic modulus, G_e, are calculated by taking the secant modulus at an axial strain interval of 0.5-1%, and the shear plastic modulus at an interval of 10-20% for PU and 30-50% for ADP adhesive. Table 13 summarizes the shear mechanical properties for the PU and ADP adhesive models. Figure 33 shows the average shear stress-strain curves for PU and ADP adhesives.

Table 13 Shear test results for PU and ADP adhesive properties

Adhesive	τ_u [MPa]	γ_u [%]	τ_e [MPa]	G_e [MPa]	G_p [MPa]
PU	20.8	40	10.0	355	42
ADP	8.3	230	3.0	33	3

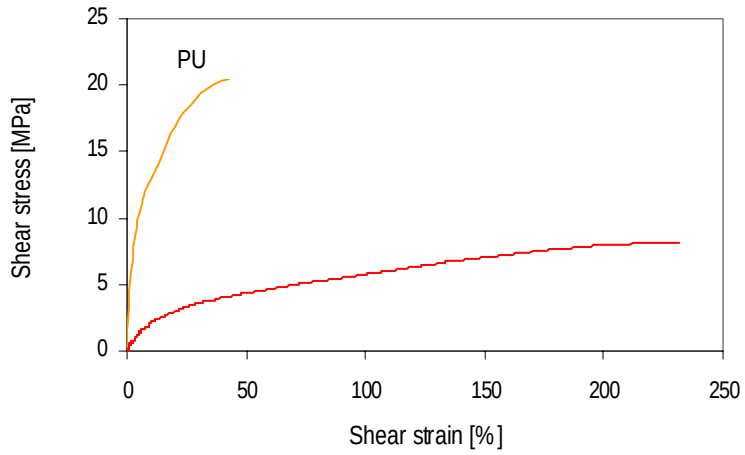

Figure 33 Average shear stress-strain curves for PU and ADP

Figure 34 EP shear specimen after failure

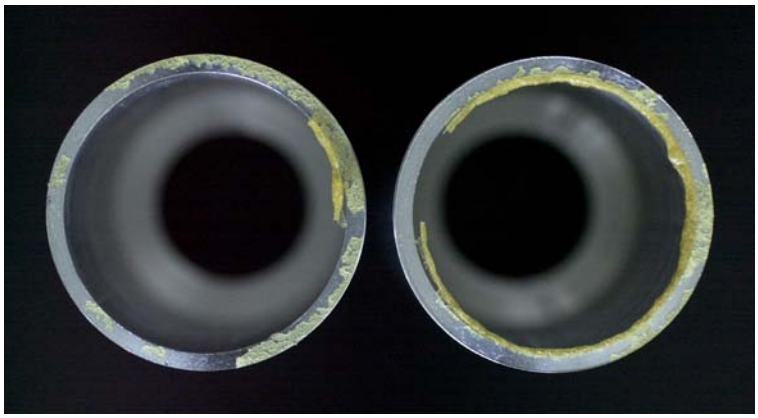

Figure 35 PU shear specimen after failure

Figure 36 ADP shear specimen after failure

5 Summary

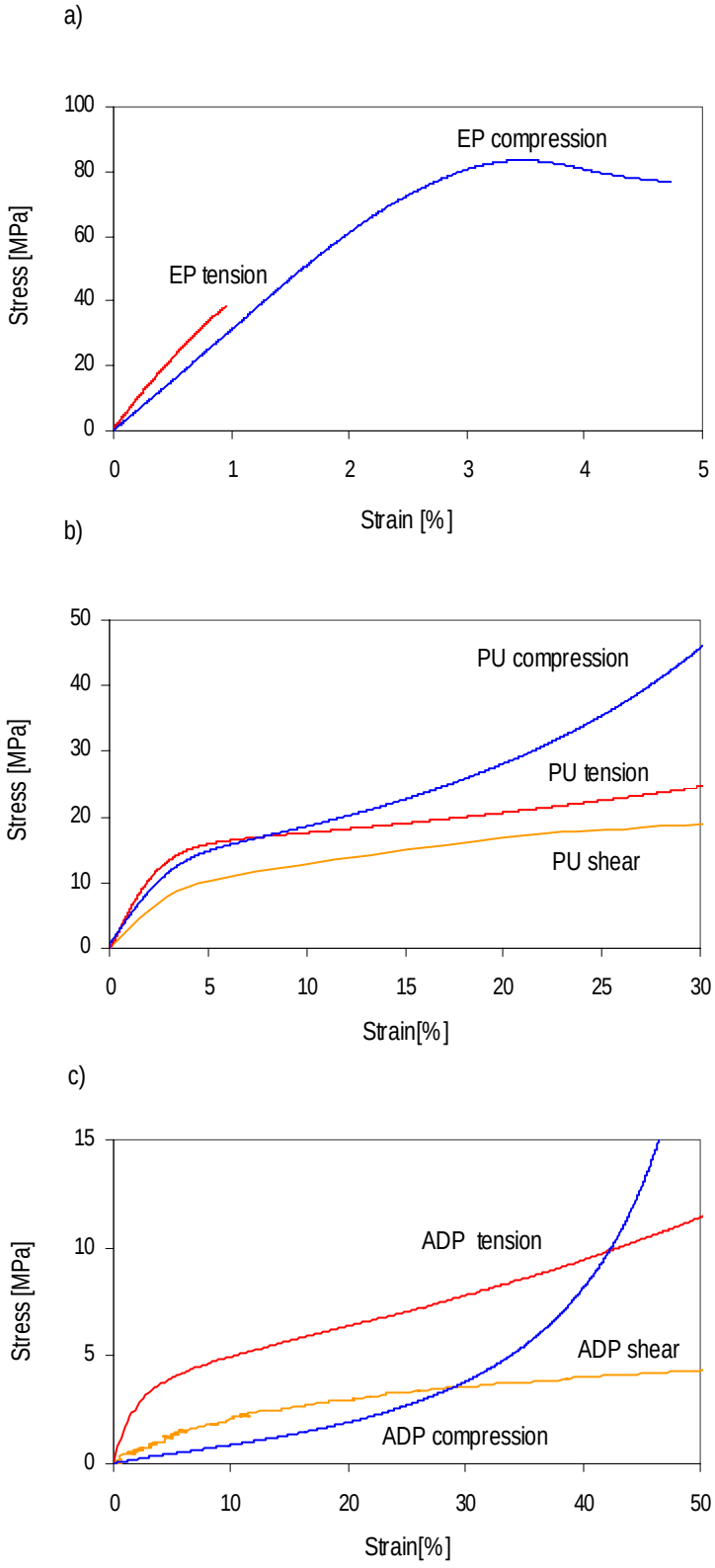

Figure 37 Average tensile, compressive and shear stress-strain curves of (a) EP, (b) PU, (c) ADP (v=5 mm/min in tension)

Figure 37 shows the average tensile, compressive and shear stress-strain curves for EP, PU and ADP adhesives. The ratio between the tensile and compressive Young's moduli is 1.5 and 1.1 for EP and PU respectively. The ratio is higher for ADP, partly due to the higher displacement rate in traction than in compression. Despite the difference between the stress-strain curves in tension and compression, its influence on joint behavior is not significant since the latter depends on the relative stiffness of the adherends and adhesive and in both cases the ratio is high (Renton and Vinson 1975).

6 Acknowledgements

The author wishes to acknowledge the support of the Swiss Innovation Promotion Agency CTI (Contract No. 4676.1), Sika AG Zurich (adhesive supplier and M. Aubert, M. Flepp, R. Jaeggi, and V. Venetz for their assistance related to the experimental aspects. She is also grateful to M. Schmid from the EMPA in Dübendorf for his contribution.

7 List of Figures

8 List of Tables

9 References

ADAMS R.D., COPPENDALE J. (1977), The Elastic Moduli of Structural Adhesives, *Adhesion*, Allen K.W. ed., Applied Science Publishers, London, United Kingdom, pp 1-17.

ADAMS R.D., COPPENDALE J. (1979), The Stress-Strain Behaviour of Axial Loaded Butt Joints, *Journal Adhesion*, Vol. 10, No. 1, pp 49-62.

ADAMS R.D., COMYN J., WAKE W.C. (1997), *Structural Adhesive Joints in Engineering*, Second Edition, Chapman & Hall, London, United Kingdom.

ATHOL W., BROCKMANN W. (1976), *New Test Methods for the Prediction of Environmental Resistance of Adhesive Bonded Joints, Bicentennial of Materials Progress*, Vol. 21, pp 581-591.

ASTM D 638-96 (1996), Standard Test Method for Tensile Properties of Plastics, *Annual Book of ASTM Standards*, Vol. 08.01, United States of America.

ASTM D 695M-96 (1996), Standard Test Method for Compressive Properties of Rigid Plastics [Metric][1], *Annual Book of ASTM Standards*, Vol. 08.01, United States of America.

ASTM D 1002-99 (1999), Standard Test Method for Apparent Shear Strength of Single-Lap-Joint Adhesively-bonded Metal Specimens by Tension Loading (Metal-to-Metal), *Annual Book of ASTM Standards*, Vol. 15.06, United States of America.

ASTM 3983-98 (2000), Standard Test Method for Measuring Strength and Shear Modulus of Nonrigid Adhesives by the Thick-Adherend Tensile-Lap Specimen, *Annual Book of ASTM Standards*, United States of America.

ASTM E 229-97 (2000), Standard Test Method for Shear Strength and Shear Modulus of Structural Adhesives, *Annual Book of ASTM Standards*, United States of America.

BASSETTI A. (2001), *Lamelles précontraintes en fibres carbone pour le renforcement de ponts rivetés endommagés par fatigue*, Dissertation ETH NO. 2440, ETH Lausanne, Switzerland.

COGNARD J.(2000), *Science et technologie du collage*, PPUR Lausanne, Switzerland.

CROCOMBE A .D., RICHARDSON G, SMITH P.A. (1993), Measuring Hydro-Static Dependent Constitutive Behaviour of Adhesives Using a Bend Specimen, *Journal Adhesion*, Vol. 42, No. 3, pp 209-223.

DE BRUYNE N.A. (1951), *Adhesion and Adhesives*, De Bruyne N.A. and Houwink R. ed., Elsevier, Amsterdam, The Netherlands, pp 92.

DE CASTRO J. (2005), *Experiments on Bonded Double-lap Joints with Epoxy, Polyurethane and Acrylic Adhesives*, Technical Report CCLab2000.1b/2, CCLab-EPFL, Lausanne, Switzerland.

DEURING M. (1993), *Verstärken von Stahlbeton mit gespannten Faserverbundwerkstoffen*, Dissertation ETH No. 10199, ETH Zürich, Switzertland.

DOLEV G., ISHAI O. (1981), Mechanical Characterization of Adhesive Layer "In Situ" and as Bulk Material, *Journal Adhesion*, Vol. 12, No. 4, pp 283-294.

EN ISO 527-1 (1996), Determination of Tensile Properties - Part 1: General Principles, *European Standard*, Brussels, Belgium.

EN ISO 527-2 (1996), Determination of Tensile Properties - Part 2: Test Conditions for Moulding and Extrusion Plastics, *European Standard*, Brussels, Belgium.

EN ISO 11003-1 (1993), Adhesives - Determination of Shear Behaviour of Structural Bonds - Part 1: Torsion Test Method Using Butt-Bonded Hollow Cylinders, *European Standard*, Brussels, Belgium.

FISCHER M., PASQUIER M.(1989), *Shear Behaviour of Structural Adhesives in the Bondline, Construction & Building Materials*, Vol. 3, No. 1, pp 31-34.

GALI S., DOLEV G., ISHAI O. (1981), An effective Stress/Strain Concept in the Mechanical Characterization of Structural Adhesive Bonding, *International Journal of Adhesion and Adhesives*, Vol. 1, No. 3, pp 135-140.

HANCOX N.L., MAYER R.M. (1994), *Design Data for Reinforced Plastics: a Guide for Engineers and Designers*, Chapman & Hall, London, United Kingdom.

HART-SMITH L.J. (1990), Joining, Mechanical Fastening, *International Encyclopedia of Composites*, Stuart M.L. ed., VCH Publisher, New York, United States of America, Vol.2, pp 438-460.

IKEGAMI K., KAJIYAMA M., KANIKO S., SHIRATORI E. (1979), Experimental Studies of the Strength of an Adhesive Joint in a State of Combined Stress, *Journal Adhesion*, Vol. 10, No. 1, pp 25-38.

ISHAI O., DOLEV G. (1981), Mechanical Characterization of Bonded and Bulk Adhesive Specimens as Affected by Temperature and Moisture, *26th National SAMPE Symposium*, Los Angeles, United States of America, pp 630-641.

JEANDRAU J.P., GROLADE D.(1985), Méthodes de calculs des assemblages collés, *Colloquium on Tendances actuelles en calcul des structures*, DRET à Bastia 6-7 novembre, France, pp 873-890.

JEANDRAU J.P. (1986), Intrinsic Mechanical Characterization of Structural Adhesives, *International Journal of Adhesion and Adhesive*s, Vol. 6, No. 4, pp 229-231.

JEANDRAU J.P. (1991), Analysis and Design Data for Adhesively-bonded Joints, *International Journal of Adhesion and Adhesives*, Vol. 11, No. 2, pp 71-79.

KASSAPOGLOU C., ADELMANN J.C. (1991), KGR-1 Thick Adherend Specimen Evaluation for the Determination of the Adhesive Mechanical Properties, *23th International SAMPE Technical Conference*, Carri R.L., Poveromo L.M. and Gauland J. ed., Vol. 23, pp 162-176.

MATTHEWS F.L., KILTY P.F., GODWIN E.W. (1982), A Review of the Strength of Joints in Fibre-Reinforced Plastics. Part 2. Adhesively-bonded Joints, *Journal of Composites*, Vol. 13, No. 1, pp 29-37.

PEPPIATT N.A. (1976), *Some Aspects of the Paraboloidal Yield Surface*, University of Bristol Internal Report, Unites Kingdom.

RAGHAVA R.S., CADDELL R.M. (1973), The Macroscopic Yield Behaviour of Polymers, *Journal of Material Science*, Vol. 8, No. 2, pp 225-232.

RENTON W.J., VINSON J.R. (1975), The Efficient Design of Adhesive Bonded Joints, *Journal of Adhesion*, Vol. 7, No. 3, pp 175-193.

SCHMID M., KIESELBACH R. (2001), Adhesive Bonding - a Challenge for Design, *Journal of the Engineering Integrity Society*, Vol. 10, pp 24-33.

SCHMID M. (2002), *New Adhesive*, EMPA Scientific Report No. 200171 e02/2, Dept. Strength and Technology, EMPA Duebendorf, Switzerland.

TONG L., STEVEN G.P. (1999), *Analysis and Design of Structural Bonded Joints*, Kluwer Academic Publishers, Massachusetts, United States of America.

VALLEE T., SIEBRECHT J. (2001), *Shear Experiments on Bonded FRP-Profiles under Static Load Part 1 : Experiments with SikaDur 330*, Technical Report CCLab2000.1a/1, CCLab-EPFL, Lausanne, Switzerland.

VAN STRAALEN I.J. (2001), *Development of Design Rules for Structural Adhesive Bonded Joints : a Systematic Approach*, Dissertation Technical University Delft, The Netherlands.

VENETZ V. (2004), personnal communication, Sika AG, Tüffenwies, Switzerland.